

國立台灣大學醫學院免疫學研究所

碩士論文

Graduate Institute of Immunology

College of Medicine

National Taiwan University

Master Thesis

CD4⁺ T 細胞以及 IFN- γ 在 Zap-70 突變鼠之自體抗體

反應所扮演的角色

Role of CD4⁺ T cells and IFN- γ in autoantibody

response in Zap70 mutant mice

研究生：林珍如

Student: Jen-Ju Jessica Lin

指導教授：孔祥智 博士

Advisor: Dr. John T. Kung

中華民國 一百零一年 七月

July 2012

Acknowledgements

首先要感謝孔祥智老師在我對人生十字路口徬徨時拉了我一把，讓我進入了免疫的領域。在研究中遇到困難時，老師總是不厭其煩的與我討論問題的癥結與解決的方法，在討論之中也常提醒我保持良好的做人與做事的態度。謝謝老師這兩年在實驗和論文上的指導。感謝伍安怡老師和李建國老師在百忙之中參加我的進度報告及口試及給予實驗上的建議。感謝芬苓學姊從我進實驗室後一直耐心的教導我實驗，在我心情低落、實驗不順利時給予鼓勵，以及不時給予生活中的關心。感謝宜婷學姐和振誠學長，總是很願意教我免疫的知識。感謝張綿和淑娟，你們像媽媽一樣的關心我的身體健康和擔心我餓肚子，謝謝你們辛苦的照顧小鼠，讓我的實驗不會開空窗。感謝蘇裕家學長，即使離開了 N609，仍然給予支持與實驗上的幫助。感謝 IMB confocal microscope facility 的李淑萍與黃淑美學姊在使用 confocal microscope 上的熱心指導。感謝 IMB FACS facility 的雅敏學姊與楊凱婷在 cell sorting 上的幫忙，讓我可以順利得到實驗所需的細胞。最後最感謝的是我的爸媽和弟弟們這兩年的支持，讓我衣食無虞的專心在研究上，在我需要休息的時候，有你們的地方就是最好的避風港。

沒有你們，我不可能順利完成這份論文。心中除了感謝還是感謝。

Abstract

An ENU-induced mutant mouse with a point mutation in the *Zap70* gene was studied. This mutant *Zap70* gene encodes a *Zap70* protein with a single C to S amino acid substitution at residue 563. This *Zap70* mutant mouse spontaneously produced autoantibody and was named “Sap” for “serum autoantibody positive.” The autoantibody response in Sap mice, as a function of age, was characterized by immunofluorescence, Western blotting, and immune complex deposition techniques. Sap mice at 5 wks of age made primarily anti-cytoplasmic autoantibodies. Sap mice over 8 wks of age, on the other hand, made predominantly anti-nuclear autoantibodies (ANA), most of which were of the IgG2a isotype. Sap mice also displayed glomeruli-associated immune complex deposition, most of which were of the IgM isotype. IgG2a ANA and immune complex deposition responses were lost in Sap-CD4-KO and Sap-IFN- γ -KO mice. Adoptive transfer of Sap CD4⁺ T cells restored the deficient ANA response in Sap-CD4-KO but not Sap-IFN- γ -KO hosts. Despite the loss of ANA, anti-cytoplasmic autoantibody response was still observed in Sap-IFN- γ -KO mice. These results clearly show the key roles played by CD4⁺ T cells and IFN- γ in the induction of the ANA response. They also implicate the importance of cells other than CD4⁺ T cells as the provider of IFN- γ in the induction of the ANA response.

中文摘要

P358 小鼠為 ENU 的誘導產生的突變小鼠，其 ZAP70 蛋白激酶中發生了單一的氨基酸置換，第 563 號半胱氨酸(cysteine)被置換成絲氨酸(serine)。此小鼠於週齡五週大即產生自體免疫抗體，故給予小鼠名稱“Sap”意指“血清抗體陽性”。此研究利用免疫螢光染色法檢測血清中的抗體和沉積在腎臟腎小球的免疫球蛋白以及西方墨點法來分析隨著時間的推移，自體抗體特性的變化。Sap 小鼠有著接近系統性紅斑狼瘡疾病的症狀，具有大量的自體抗體在血清內和免疫複合物沉積在腎絲球中。Sap 小鼠在週齡五週大時主要產生抗胞質抗體，週齡八週以上主要產生抗核抗體，隨著年齡變化，Sap 小鼠增加自體抗體總量和認識的抗原種類。抗核抗體主要屬於 IgG2a 亞類，而形成的免疫複合物多數為 IgM。在 $CD4^+$ T 細胞及 γ -干擾素缺失的 Sap 小鼠中，IgG2a 抗核抗體的消失和免疫複合物沉積量降低，證明了 $CD4^+$ T 細胞及 γ -干擾素在 Sap 小鼠的自身免疫反應的重要性。將 Sap 小鼠的 $CD4^+$ T 細胞過繼轉移(adoptive transfer)至 Sap- $CD4$ -KO 小鼠體內可成功誘導抗核抗體的產生但是若過繼轉移至 Sap- IFN - γ -KO 小鼠體內則無法產生抗核抗體，然而仍然可見抗胞質抗體。此研究證明了 $CD4^+$ T 細胞和 γ -干擾素在誘發抗核抗體反應中扮演重要角色，並提供了除了 $CD4^+$ T 細胞以外由其他細胞提供 γ -干擾素主要來源的可能性。

Table of Contents

Acknowledgements	i
Abstract	ii
中文摘要	iii
Introduction	1
Materials and Methods	9
2.1 Mice	9
2.2 Cell lines	9
2.3 Autoantibody Immunofluorescence staining	10
2.4 Autoantibody detection using frozen tissues	12
2.5 Mitochondria staining	13
2.6 Western blot	14
2.7 Immunofluorescence staining of frozen tissues	16
2.8 Histological analysis	17
2.9 Anti-CD4 Treatments	18
2.10 Surface marker expression analysis by flow cytometer (FACS)	19
2.11 Spleen CD4⁺ T cell isolation by panning	20
2.12 Electronic cell sorting	21
2.13 Adoptive Transfer	22
2.14 Tracing of Donor cell persistence by flow cytometry	22
Results	24
3.1 Sap mice produce autoantibody	24
3.2 Assorted autoantibody reactivity in Sap sera as a function of age	26
3.3 Glomerular deposits of Ig developed at early age in Sap mice	28
3.4 Presence of predominant IgG2a, IgG1, but not IgM anti-nuclear autoantibody	29
3.5 Renal immune complex deposits were mostly IgM type	30
3.6 CD4⁺ T cells are required for germinal center reaction in Sap mice ...	31
3.7 IFN-γ-dependency of autoantibody response in Sap mice	33
3.8 Reduced Ig deposits in the absence of IFN-γ	33
3.9 Predominance of IgG1 and IgG2b subclasses of anti-cytoplasmic autoantibodies in Sap-IFN-γ-KO mice	34
3.10 Sap CD4⁺ T cells can reconstitute anti-nuclear autoantibody response in Sap-CD4-KO mice but not in Sap-IFN-γ-KO	34
3.11 Autoantibody response in Sap mice is partially dependent on NKT cells but not CD8⁺ T cells	36
Discussion	39

4.1	Characterization of autoantibody production in Sap mice	39
4.2	Non-CD4⁺ T cell source of IFN-γ in autoantibody production.....	43
4.3	Autophagy and ANA response.....	46
4.4	Immune complex deposition in Sap kidney without glomerulonephritis	47
	References.....	50
	Figures	59



Introduction

P358 ENU-mutagenized mice with Zap70 mutation

CD3 zeta-chain associated protein, Zap70, is a downstream tyrosine kinase of the TCR signaling pathway. It is essential for TCR signal transduction and has been shown to play critical roles in T cell development and activation (Au-Yeung et al., 2009). P358 is an ENU mutant mouse line that has a T to A point mutation in the Zap70 gene that corresponds to a cysteine to serine change at amino acid position 563 in the C-terminal kinase domain. Due to the readily detectable autoantibodies in the serum of P358 mice, we have named P358 C563S allele “*Sap*” for “serum autoantibody positive”. Previous work in our laboratory by Wei-Ching Hsu has shown that *Sap* Zap70 protein turns over more rapidly than WT Zap70, has impaired kinase activity, and fails to phosphorylate Lat, its downstream substrate.

Known Zap70 missense mutations

Differential TCR signaling transduction can induce diverse autoimmune syndromes as a consequence of different positive or negative selection (Hsu et al., 2009). In recent years, there have been reports on several hypomorphic Zap70 allelic mutant mice.

SKG mice, a known animal model resembling human rheumatoid arthritis, carry a

point mutation W163P in the C-terminal SH2 kinase domain (Sakaguchi et al., 2003). SKG mice develop arthritis in the BALB/c background in a conventional condition but are resistant to arthritis when raised on the C57BL/6 background (Sakaguchi et al., 2003; Sakaguchi and Sakaguchi, 2005). Furthermore, it has been found that under a specific pathogen free (SPF) environment, SKG mice are insusceptible to arthritis unless challenged with zymosan (Hsu et al., 2009; Yoshitomi et al., 2005). SKG mice spontaneously develop hypergammaglobulinemia, a high titer of rheumatoid factor (RF), a type II collagen specific autoantibody (CII), and autoantibody against heat shock protein-70 (HSP-70) (Sakaguchi et al., 2003). Joint swelling and CD4⁺ T cell infiltration to the subsynovial tissue are accompanied with the disease. In addition, SKG mice exhibit weak TCR signaling strength to a greater extent resulting in a positive selection of self-reactive T cells and a more defective negative selection during T cell development (Hsu et al., 2009; Sakaguchi et al., 2003).

More recently, a hypomorphic Zap70 allele T3 is induced by ENU-mutagenesis carried out on a C3H background. E589G mutation as a result of a single nucleotide A to G transition leads to a complete block of T cell development at double positive stage (Jakob et al., 2008). T3 mice display normal Zap70 mRNA expression but reduced Zap70 protein level. The mutant is found to have an increased plasma IgE level. However, T3 mice do not display clinical symptoms of autoimmune disease, RF, or

anti-DNA autoantibodies (Jakob et al., 2008).

P358 mice, in contrast, develop autoantibodies but not arthritis, a phenotype that is similar to *Zap70^{mrt/mrd}* mice (Siggs et al., 2007). *Zap70^{mrt/mrd}* mice are generated by crossing *Zap70^{mrd/mrd}* and *Zap70^{mrt/mrt}* mutant mice. The *mrd* and *mrt* *Zap70* alleles carry I367F and W504F amino acid changes, respectively. The *mrt* allele results in 75% reduction in *Zap70* protein expression while *mrd* allele does not alter *Zap70* protein expression. Neither alleles result in hyper IgE or autoimmune disease. On the other hand, *Zap70^{mrt/mrd}* mice exhibit diminished peripheral CD4⁺ T cells but normal numbers of CD8⁺ T cells compared to WT mice (Siggs et al., 2007). The reduced TCR signal strength due to defective *Zap70* expression is responsible for the impaired thymic negative selection and altered immunosuppressive properties of CD4⁺Foxp3⁺ cells. In addition, *Zap70^{mrt/mrd}* mice spontaneously secrete anti-nuclear or anti-cytoplasmic autoantibodies and high level of IgG1 and IgE (Siggs et al., 2007). In our laboratory, we have previously found that CD4⁺ cells are reduced by 4- and 2- folds in the thymus and the spleen of Sap mice, respectively, but the level of CD8⁺ cells is unaffected (done by Fen-Ling Chen). Sap mice also exhibit anti-nuclear and anti-mitochondrial autoantibodies in addition to elevated IgG and IgE levels (done by Jessica Lin and Fen-Ling Chen). Although the number of CD4⁺CD25⁺ Treg cells has a 7-fold decrease in the thymus compared to WT mice, these cells display normal *in vitro* but impaired *in*

vivo suppressive function (done by Fen-Ling Chen and Wei-Ching Hsu).

Autoimmune response, autoantibody patterns, and detection methods

Autoimmune response initiates when tolerance against self-antigens becomes dysregulated. Factors leading to autoantibody productions include breakdown of B and T cell tolerance, abnormal presentation of autoantigens, and defects in clearance of apoptotic cells; for example, MRL/lpr mice carrying mutation on the *lpr* gene show defective deletion of peripheral autoreactive T cells which leads to lupus-like diseases marked by autoantibody generation and kidney pathogenesis (Singer and Abbas, 1994; Watanabe-Fukunaga et al., 1992). That being said, the presence of autoantibodies, immunoglobulins that target self-antigens, is a sign of breakdown of self-tolerance. Autoantibodies are of diagnostic value and are involved in most autoimmune diseases. However, they arise not only from patients with autoimmune diseases but also from healthy individuals. It has been reported that anti-nuclear autoantibodies (ANA) are seen in healthy people and the prevalence of ANA increases with age without clinical signs of diseases (Xavier et al., 1995). The autoreactivity is found greater in women than in men. Furthermore, autoantibodies are detectable in patients several years before and subsequently develop system lupus erythematosus (SLE) (Eriksson et al., 2011).

In Sap mice, the attenuated Zap70 expression results in serum autoantibodies

without developing into autoimmune symptoms. Anti-nuclear and anti-mitochondria autoantibodies are two distinct autoantibody patterns in Sap serum. Autoantibodies that recognize nuclear components such as the nucleosomes and histones are categorized as ANA, mostly found in autoimmune diseases (Bertry-Coussot et al., 2002). Anti-mitochondrial antibodies (AMA) are the major autoantibodies found in primary biliary cirrhosis (PBC) (Mackay, 1958). However, the presence of anti-mitochondrial antibodies is not necessarily associated with disease (Mattalia et al., 1998). AMA can coexist with other type of antibodies such as anti-nuclear and anti-cytoplasmic autoantibodies (Gershwin et al., 1988).

ANA are imperative clinical biomarkers for diagnosis and classification of autoimmune diseases (Wiik et al., 2010). Various methods can be used to detect autoantigens in autoimmune disease. Assays such as immunofluorescence using frozen sections of rat liver or kidney or Hep-2 cells, and western blotting (WB) are commonly performed although their degree of sensitivity and specificity varies (Benson et al., 2004; Miyakawa et al., 2001). WB has its advantage over IF with high sensitivity and precision in providing information on possible molecular targets, whereas IF is a better method for visualizing the distribution and localization of specific cellular protein and is less time consuming.

Germinal center and autoantibody production

One of the hallmarks in the production of autoantibody is the formation of germinal centers (GCs) in the spleen of autoimmune or infected mice. Spontaneous GC reactions have been reported in various autoimmune models (Luzina et al., 2001). GC reactions are highly dependent on T helper (Th) cells. $CD4^+$ Th cells are the major cell subset that initiates T-B cell interaction at the follicular border which in turn promotes B cell proliferation and subsequently, the GC formation. In recent years, a specific $CD4^+$ T cells that localized in B cell follicles, the follicular T helper cells (T_{FH}), have been identified. Together with follicular dendritic cells, T_{FH} cells stimulate somatic hypermutation and facilitate affinity maturation of GC B cells (Goodnow et al., 2010). In addition, Ig class switch recombination is strongly influenced by cytokines. IL-4 promotes IgG1 and IgE isotype switch whereas IFN- γ promotes IgG2a isotype switch (Kalinski and Moser, 2005).

B cells develop into antibody-secreting cells in two different ways. After B cells are activated by helper T cells, they differentiate into GC B, circulating memory B, or extrafollicular plasma B cells (Goodnow et al., 2010). Circulating memory B and extrafollicular plasma B cells capable of producing IgG do not undergo immunoglobulin class switch and affinity maturation, and thus are short-lived. Alternatively, GC B cells that migrate into GC further differentiate into long-lived

memory B cells and plasma B cells that persistently produce autoantibodies into blood (Goodnow et al., 2010). This may be the case for Sap mice since they continuously generate autoantibodies throughout life.

Immune complex kidney deposition and glomerulonephritis

Autoimmune response also happens in the kidney. Immune complex mediated tissue damage is one pathogenic mechanism of autoantibodies commonly seen in autoimmune diseases such as system lupus erythematosus (SLE) (Weening et al., 2004). In the kidney, immune complexes usually deposit in the glomerular cells (mesangial cells) and Bowman's capsule. Circulating autoantibodies bind to antigens, forming immune complexes that deposit in the glomeruli and damage kidney filters. This is accompanied by the development of proteinuria that can be measured by albumin:creatinine ratio (Hemmelgarn et al., 2010). Kidney failure further leads to serious illness and death. In most SLE animal models, predominantly IgG and C3 complement deposition is found (Waldman and Madaio, 2005). Furthermore, IgG anti-dsDNA autoantibodies have been shown to be associated with glomerulonephritis (Kotzin, 1996). Interestingly, high levels of IFN- γ secreted by CD4⁺ T cells in MRL/lpr mice have been shown to be responsible for IgG autoantibodies and renal damage (Balomenos et al., 1998; Haas et al., 1998). In order to accommodate an accurate

guideline for diagnostic purposes, the World Health Organization (WHO) in 1982 and the International society of Nephrology/Renal Pathology Society (ISN/RPS) in 2003 have formulated classification of lupus nephritis (Weening et al., 2004). Whether Sap mice develop glomerulonephritis is still not known given that they do not seem to have apparent kidney problems.

Here I report in this study an observation on the intensity and pattern changes of autoantibody reactivities against cell organelles over time in Sap mice that carry a point mutation in Zap70 gene. The study also demonstrates that autoantibodies are produced in a CD4⁺ T cells and IFN- γ dependent manner. The major aim of the study is to elucidate how a point mutation on Zap70 gene leading to defective TCR signaling that further impacts on immune response. We expect these results to provide credible insights into underlying mechanisms linking attenuated Zap70 expression and autoantibody response in Sap mice.

Materials and Methods

2.1 Mice

C57BL/6

Zap70^{Sap/Sap} (Sap), ENU-mutagenized mice Pedigree 358

Sap-CD1d-KO

Sap-IFN- γ -KO

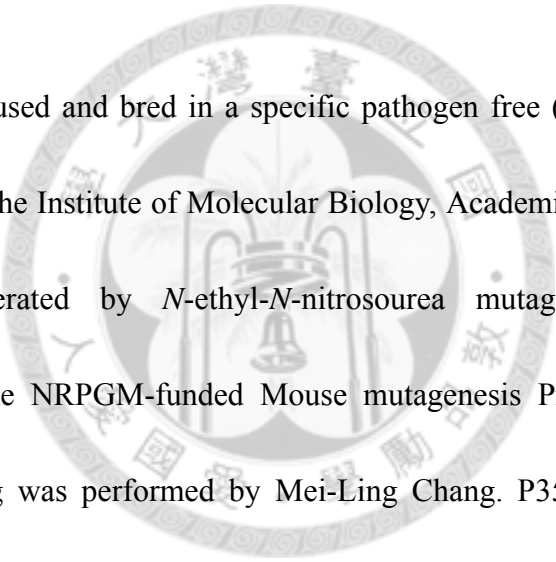
Sap-TCR β -KO

Sap-CD4-KO

Sap-CD8-KO

Sap-KOII

IgH-KO



All mice were housed and bred in a specific pathogen free (SPF) condition in the animal facility at the Institute of Molecular Biology, Academia Sinica. P358 mutant mice were generated by *N*-ethyl-*N*-nitrosourea mutagenesis on C57BL/6 background by the NRPGM-funded Mouse mutagenesis Program Core Facility. Mutation mapping was performed by Mei-Ling Chang. P358 mice were crossed with CD1d-KO, IFN- γ -KO, TCR β -KO, CD4-KO, CD8-KO, and KOII mice to generate Sap-CD1d-KO, Sap-IFN- γ -KO, Sap-TCR β -KO, Sap-CD4-KO, Sap-CD8-KO, and Sap-KOII mice, respectively. All mice were used between 4 to 41 weeks of age.

2.2 Cell lines

B16-F10 melanoma cells were maintained in Dulbecco's modified Eagle's medium

(DMEM) growth medium supplemented with 10% FBS at 37 °C in 5% CO₂.

2.3 Autoantibody Immunofluorescence staining

A. Reagents

DMEM+10% FBS

DMEM	Gibco 12100-038
1 M HEPES (pH7.3)	20 ml/L
7.5% Sodium Bicarbonate	50 ml/L
100 nM Sodium Pyruvate	10 ml/L
FBS (Heat inactivated at 56 °C for 30 minutes)	100 ml/L
100x Penicillin + streptomycin	(Gibco 15140-122) 10 ml/L

1 X PBS pH7.4

Sodium Chloride	54.8 mM/L
Potassium Chloride	1.1 mM/L
Disodium Phosphate	3.2 mM/L
Monopotassium Phosphate	0.6 mM/L

PBS + 5% FBS

Collagen I, rat tail **BD 354236**

0.2% Triton X-100 in 1x PBS

EM grade 16% Paraformaldehyde fixative **Electron Microscopy Sciences**

Faramount Aqueous Mounting Medium **DAKO S3025**

B. Antibodies

	<u>Clone</u>
Biotin rat anti-mouse IgG1 mAb	(BD Bioscience) A85-1
Biotin rat anti-mouse IgG2a mAb	(BD Bioscience) R19-15
Biotin rat anti-mouse IgE mAb	(BD Bioscience) R35-18
Biotin rat anti-mouse IgA mAb	(BD Bioscience) C10-1
Biotin rat anti-mouse IgG2b mAb	(BD Bioscience) R12-3
Biotin rat anti-mouse IgG3 mAb	(BD Bioscience) R40-82
A488 rat anti-mouse IgM mAb	Bet2
A488-Streptavidin (A488-SA)	
A488 goat anti-mouse Ig	
Hoechst 33342	

C. Procedure

B16-F10 melanoma cells were grown in tissue culture (DMEM + 10% FBS). To detect the presence of autoantibodies, B16-F10 melanoma cells were trypsinized (0.05% Trypsin-EDTA), washed with PBS, and cultured on coverslips pre-coated with collagen I for 24 hours. Prior to the immunocytochemistry procedure, cells were washed briefly in PBS before fixing with 4% PFA for 10 minutes and washed with PBS three times, 5 minutes each. Cells were permeabilized with 0.2% Triton X-100, blocked with 5% FBS in PBS, and incubated with mouse serum (1:500 dilution) in PBS + 5% FBS for one hour at room temperature. After washing with PBS three times, 5 minutes each, cells were incubated with A488 goat anti-mouse Ig (1:100 dilution, 2 $\mu\text{g}/\text{ml}$) or A488 rat anti-mouse IgM (1:200 dilution, 1 $\mu\text{g}/\text{ml}$) in PBS + 5% FBS for one hour or biotin rat anti-mouse IgG1, IgG2a, IgE, IgA, IgG2b, or IgG3 (1:500 dilution, 1 $\mu\text{g}/\text{ml}$) in PBS + 5% FBS overnight at 4 °C. Cells stained with biotin-conjugated monoclonal antibodies were sequentially stained with A488-SA (1:100 dilution, 1 $\mu\text{g}/\text{ml}$) in PBS + 2% dFBS for 3 hours at room temperature. After PBS wash 3 times, five minutes each, cells were counterstained with Hoechst 33342 for 10 minutes (1:500 diluted, 2 μM) at room temperature. Coverslips were mounted onto slides. Images were obtained by LMS 510 META Confocal Laser Scanning Microscope (Carl Zeiss) at 630x magnification, 2x zoom.

2.4 Autoantibody detection using frozen tissues

A. Reagents

1 X HBSS (Hank's balanced salt solution) + 5% FBS

HBSS	Gibco/BRL No. 61200-036
1 M HEPES (pH7.3)	20 ml/L
FBS (Heat inactivated at 56 °C for 30 minutes)	50 ml/L

1 X PBS pH7.4

0.2% Triton X-100 in 1x PBS

EM grade 16% Paraformaldehyde fixative	Electron Microscopy Sciences
Faramount Aqueous Mounting Medium	DAKO S3025

B. Antibodies

A488 goat anti-mouse IgG
Hoechst 33342

C. Procedure

Livers or kidneys were harvested from IgH-KO mice, placed in embedding medium (Sakura Finetek Tissue-Tek O.C.T. Compound), and snap-frozen in n-hexane. 5 μ m sections were cut with a cryostat and air-dried. The sections were fixed with 4% PFA for 10 minutes, rinsed with 1x PBS twice, 10 minutes each, followed by permeabilization with 0.2% Triton X-100 for 5 minutes at room temperature. After washing the slides with 1X PBS twice, 10 minutes each, non-specific antibody binding sites were blocked with HBSS + 5% FBS for 30 minutes at room temperature followed by incubation with mouse serum (1:500 dilution) in HBSS + 5% FBS at 4 °C overnight. After washing with PBS twice, 10 minutes each, the slides were incubated with A488-conjugated

anti-mouse Ig (1:100 diluted, 2 μ g/ml) in HBSS + 5% FBS for one hour at room temperature. After 1xPBS wash twice, 10 minutes each, the sections were counterstained with Hoechst 33342 for 10 minutes (1:500 diluted, 2 μ M) at room temperature. Coverslips were mounted onto slides after a quick wash with 1x PBS. Samples were analyzed with LMS 510 META Confocal Laser Scanning Microscope (Carl Zeiss) at 200x or 630x magnification.

2.5 Mitochondria staining

A. Reagents

DMEM+10% FBS

1 X PBS pH7.4

PBS + 5% FBS

0.05% Trypsin-EDTA

Collagen I, rat tail

0.2% Triton X-100 in 1x PBS

MitoTracker Deep Red FM

EM grade 16% Paraformaldehyde fixative

Faramount Aqueous Mounting Medium

Gibco 25300-054

BD 354236

Molecular Probes

Electron Microscopy Sciences

DAKO S3025

B. Antibodies

A488 goat anti-mouse Ig

Hoechst 33342

C. Procedure

B16-F10 melanoma cells were grown in tissue culture (DMEM + 10% FBS). To detect the presence of autoantibodies, B16-F10 melanoma cells were trypsinized (0.05%

Trypsin-EDTA), washed, and cultured on coverslips pre-coated with collagen I for 24 hours. Mitochondria were stained with 200 nm MitoTracker Deep Red FM in DMEM + 10% FBS at 37 °C for 35 minutes. After washing with PBS, the cells were fixed with 4% PFA in PBS + 5% FBS at 37 °C for 15 minutes. The cells were washed with PBS three times, 5 minutes each, permeabilized with 0.2% Triton X-100 for 5 min, and blocked with PBS + 5% FBS for 30 minutes at room temperature. Mouse serum (1:500 dilution) in PBS + 5% FBS was added to the fixed B16-F10 cells and incubated at room temperature for one hour followed by PBS wash and incubation with A488-conjugated anti-mouse Ig (1:100 diluted, 2 µg/ml) in PBS + 5% FBS for one hour at room temperature. After washing with PBS three times, 5 minutes each, cells were counterstained with Hoechst 33342 for 10 minutes (1:500 dilution, 2 µM) at room temperature. Cells were visualized by LMS 510 META Confocal Laser Scanning Microscope (Carl Zeiss) at 630x magnification, 2x zoom.

2.6 Western blot

A. Reagents

1x RIPA lysis buffer

Tris-HCl pH7.5	50 mM/L
Sodium Chloride	150 mM/L
NP-40	1%
Deoxycholate (DOC)	0.5%
SDS	0.1%

6x SDS sample buffer

1M Tris-HCl pH6.8	3.5 ml
Glycerol	3.0 ml
SDS	1g

10X TBST

2M Tris-HCl pH7.4	100 mM
5M NaCl	1.5 M
Tween-20	0.5%

WesternBright ECL detection kit**Advansta****Prestained Protein Ladder****Fermentas****Bio-Rad Protein Assay****Bio-Rad****B. Antibodies**

HRP goat α -mouse IgG Jackson ImmunoResearch (#115-035-003)

C. Procedure

IgH-KO mouse livers were lysed with ice-cold 1x RIPA lysis buffer containing protease and phosphatase inhibitor mixture (Sigma) for 20 minutes on ice. Lysates were obtained after centrifugation at 400 rcf for 10 minutes at 4 °C. The protein concentration was determined with Bio-Rad Protein Assay using BSA as a standard. Lysates were mixed with 6X SDS sample buffer and heated to 95 °C for 5 minutes. 1.3 mg protein samples and prestained protein ladder were separated by 8% SDS-PAGE, electrotransferred on nitrocellulose membranes (PerkinElmer), and blocked with 5% skim milk in 1x TBST for one hour at room temperature. The blots were clamped between the gasket and the sample template of the BIO-Rad mini-PROTEAN II multiscreen apparatus, incubated with mouse sera (1:160 dilution) overnight at 4 °C, and washed with 1x TBST three

times, 5 minutes each. Immunodetection was done by incubating membranes with HRP goat anti-mouse IgG (1:5000 dilution) for one hour at room temperature. The blots were washed with 1x TBST twice, 10 minutes each, and developed with chemiluminescence WesternBright ECL detection kit.

2.7 Immunofluorescence staining of frozen tissues

A. Reagents

Acetone

1 X HBSS (Hank's balanced salt solution) + 5% FBS

1 X PBS pH7.4

Dialyzed FBS (dPBS)

Faramount Aqueous Mounting Medium

DAKO S3025

B. Antibodies

	<u>Clone</u>
A488 goat anti-mouse Ig	
A488-streptavidin (A488-SA)	
A488 rat anti-mouse IgM mAb	Bet2
Biotin rat anti-mouse IgG2a mAb	(BD Bioscience) R19-15
Biotin rat anti-mouse IgG1 mAb	(BD Bioscience) A85-1
A546-B220 mAb	6B2
A488-Thy1.2 mAb	30H12
A488-GK1.5 mAb	GK1.5
A647-GL7 mAb	(BD Bioscience) GL7

C. Procedure

Kidneys or spleens from mice were harvested, placed in embedding medium (Sakura Finetek Tissue-Tek O.C.T. Compound), and snap-frozen in n-hexane. 5- μ m thick sections were cut with a cryostat and air-dried. The sections were fixed in ice-cold

acetone for 10 minutes, washed with 1x PBS twice, 10 minutes each, followed by A488 goat anti-mouse Ig, A488 rat anti-mouse IgM, or biotin rat anti-mouse IgG1 or IgG2a monoclonal antibodies (1 µg/ml) plus 2.4G2 Fc receptor block in HBSS + 5% FBS at 4 overnight to detect immune complex deposition. Sections stained with biotin-conjugated monoclonal antibodies were washed with PBS and subsequently stained with A488-SA (1:100 dilution, 1 µg/ml) in PBS + 2% dFBS for 3 hours at room temperature. For germinal center (GC) analyses, acetone fixed spleen sections after rinsing with PBS were stained with A564-B220, A488-GK1.5 or A488-Thy1.2, and A647-GL7 monoclonal antibodies (1 µg/ml) at 4 overnight. After 1x PBS wash twice, 10 minutes each, all sections were counterstained with Hoechst 33342 for 10 minutes (1:500 dilution, 2 µM) at room temperature. Coverslips were mounted onto slides. Sections were visualized by LMS 510 META Confocal Laser Scanning Microscope (Carl Zeiss) at 100X, 200X, 400X, or 630x magnification. Quantitative measurements of the size of GCs were carried out using Integrated Morphometry Analysis function of Metamorph software.

2.8 Histological analysis

A. Reagents

Harris Hematoxylin solution

Eosin

0.3% Acid alcohol (37% HCl in 70% ethanol)

Sigma-Aldrich HHS16

Leica Microsystems

Ethanol
Xylenes
Malino mounting medium

Merck
J.B. Baker
Muto Pure Chemicals Co. Ltd.

B. Procedure

Kidneys from mice were harvested, placed in embedding medium (Sakura Finetek Tissue-Tek O.C.T. Compound), and snap-frozen in n-hexane. 5- μm thick sections were cut with a cryostat and air-dried. Sections were stained with hematoxylin for 2 minutes and washed with tap water. The sections were differentiated with 0.3% acid alcohol for 3 seconds followed by washing with tap water, counterstained with eosin for 7 minutes, and washed with tap water. The sections were then dehydrated in the following ethanol series: 70%, 95%, and 100% two times, one minute each, then immersed in xylenes two times, one minute each. Stained slides were mounted with Malino mounting media and examined. Images were taken with Zeiss AxioZ1 Imager microscope at 400x magnification. The glomerular size was measured by ZEN 2009 light edition.

2.9 Anti-CD4 Treatments

A. Antibodies

Anti-CD4 mAb

Clone GK1.5

B. Procedure

Four 12-week-old male Sap mice were intravenously injected with 200 μg anti-CD4

mAb on day 0. The treated mice were sacrificed one at a time on days 2, 4, 7, and 10. For repeated treatment, one 12-week-old male Sap mice were intravenously injected with 200 µg anti-CD4 mAb on days 0 and 4 and sacrificed on day 9. Spleens were harvested from the mice and weighed. One-third of the spleen was used for single cell suspension and flow cytometry analysis. The remaining two-thirds of the spleen was subjected to be embedded in OCT and analyzed for splenic GCs.

2.10 Surface marker expression analysis by flow cytometer (FACS)

A. Reagents

1xHBSS (Hank's balanced salt solution) + 5% FBS

HBSS	Gibco/BRL No. 61200-036
1 M Hepes (pH7.3)	20 ml/L
FBS (Heat inactivated at 56 °C for 1 hour)	50 ml/L

Propidium iodide (PI)

Sigma No. P-9144, 1 µg/ml

1xACK lysis buffer

Ammonium Chloride	775 mM/L
Potassium Bicarbonate	50 mM/L

B. Monoclonal Antibody

<u>Conjugated mAb</u>	<u>Clone</u>
A405- α -CD8	53-6.7
A488- α -CD4	GK1.5
A647- α -TCR β	H57.597
Fc receptor blocker	2.4G2
PE-CD4	GK1.5
A647- α -B220	6B2
A647- α -NK1.1	PK136
A647- α -IgM	Bet2

C. Procedure

Spleens were harvested and teased with forceps to release single cells. The single cell suspension was passed through a cotton plug to eliminate coarse debris. After centrifugation, the cell pellet was treated with 5 ml ACK lysis buffer to lyse RBCs, centrifuged, and resuspended in HBSS + 5% FBS. The obtained lymphocytes were stained with conjugated monoclonal antibodies plus 2.4G2 to block non-specific binding of mAb to Fc receptor for 20 minutes on ice. Cells were then washed with ice-cold HBSS + 5% FBS once, resuspended in 300 μ l PI, and analyzed with flow cytometry LSRII (BD Bioscience). Data were analyzed using the FlowJO software (Tree Star, Inc.). For cell sorting, Ig⁺ and CD8⁺ cell-depleted spleen cells were stained with A647- α -B220, A647- α -NK1.1, A647- α -IgM, PE- α -CD4, and 2.4G2 and incubated on ice for 20 min. Cells were washed with ice-cold HBSS + 5% FBS once, resuspended in 2 ml ice-cold PI (1 μ g/ml), and analyzed by fluorescence activated cell sorter.

2.11 Spleen CD4⁺ T cell isolation by panning

A. Reagents

1xHBSS (Hank's balanced salt solution) + 5% FBS

1xPBS pH7.4

1xACK lysis buffer

B. Monoclonal Antibody

<u>Conjugated mAb</u>	<u>Clone</u>
Anti-mouse μ chain	Bet 2
Anti-mouse κ chain	187.1
Anti-mouse CD8	3.155

C. Procedure

Splenic lymphocytes were prepared as described in 2.10. Single cell suspension from mouse spleens was depleted of Ig⁺ cells by adherence to culture plates coated with 25 µg anti-Igµ chain mAb and 25 µg anti-Igκ chain mAb at room temperature for 50 min. Non-adherent cells were then collected and added to culture plate that had been coated with 3 µg of anti-CD8 mAb at room temperature for 30 min. To obtain CD4⁺ T cells, nonadherent cells (Igµ⁻Igκ⁻CD8⁻ splenocytes) were recovered and washed with HBSS + 5% FBS. Purified CD4⁺T cells were always >95% CD4⁺.

2.12 Electronic cell sorting

A. Reagents

1xHBSS (Hank's balanced salt solution) + 5% FBS

1xPBS pH7.4

Propidium iodide (PI)

Sigma No. P-9144, 1 µg/ml

MD (Mishell-Dutton) medium + 5% FBS

MEM

Gibco 41500-034

7.5% NaHCO₃

30 ml/L

1M HEPES pH7.3

50 ml/L

2-ME (0.195 ml 2-ME in 50 ml PBS)

Sigma NO. M-3184 1 ml/L

100x Penicillin + streptomycin

(Gibco 15140-122) 10 ml/L

FBS (heat inactivated at 56 °C for 1 hour)

50 ml/L

B. Procedure

Electronic cell sorting was performed on a fluorescence-activated cell sorter (BD FACS Aria SORP) at a triggering rate of 1000 to 1500 cells/second and drop drive frequency

about 15000 drops/second. The purity of the sorted cells was monitored by reanalysis and always exceeded 98%.

2.13 Adoptive Transfer

A. Reagents

1xHBSS (Hank's balanced salt solution)

BD Insulin syringe

BD No. 328818

B. Procedure

Total spleen cells or purified CD4⁺ T cells were collected and washed with HBSS three times. Recipient mice were exposed to light for distending tail veins. Cell suspensions were intravenously injected into recipient mice along tail veins. Sap-CD4-KO mice received 1×10^7 Sap CD4⁺ T cells/mouse or 1×10^7 B6 CD4⁺ T cells/mouse. Sap-IFN- γ -KO mice received 8×10^7 Sap total spleen cells/mouse or 8.5×10^6 Sap CD4⁺ T cells/mouse.

2.14 Tracing of Donor cell persistence by flow cytometry

A. Reagents

1xHBSS (Hank's balanced salt solution)

1xHBSS (Hank's balanced salt solution) + 5% FBS

1xACK lysis buffer

Propidium iodide (PI)

Sigma No. P-9144, 1 μ g/ml

B. Monoclonal Antibody

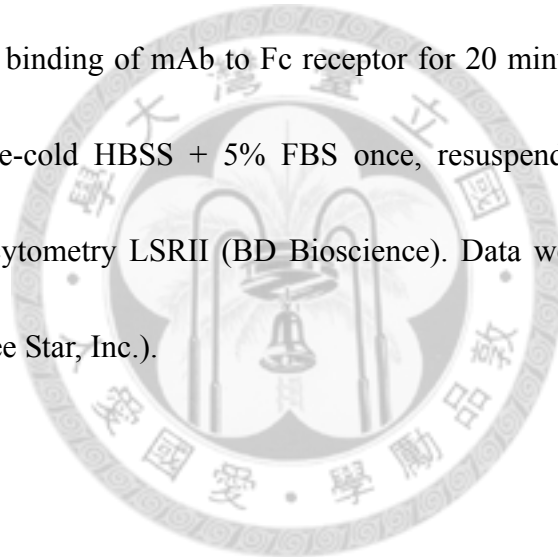
<u>Conjugated mAb</u>	<u>Clone</u>
PE- α -CD4	GK1.5

A647- α -TCR β
A405-CD8

H57.597
53-6.7

C. Procedure

Blood samples of recipients were collected into 15 ml tubes containing 12 ml ACK lysis buffer on d-1, d7, d14, and d21. After centrifugation, the cell pellet was resuspended with 10 ml ACK to lyse RBCs, centrifuged, and resuspended in HBSS + 5% FBS. The obtained lymphocytes were stained with conjugated monoclonal antibodies plus 2.4G2 to block non-specific binding of mAb to Fc receptor for 20 minutes on ice. Cells were then washed with ice-cold HBSS + 5% FBS once, resuspended in 300 μ l PI, and analyzed with flow cytometry LSRII (BD Bioscience). Data were analyzed using the FlowJO software (Tree Star, Inc.).



Results

3.1 Sap mice produce autoantibody

The presence of autoantibodies in serum samples from Sap and control B6 mice was examined by staining fixed B16-F10 tissue culture cells. At a relatively young age of 5 wks, clearly detectable but weak anti-cytoplasmic autoantibodies were seen in all four Sap (2M, 2F) mice tested (Figure 1). Co-localization of the cytoplasmic staining with MitoTracker Deep Red FM, a known mitochondria marker, indicated that most of the anti-cytoplasmic antibodies were mitochondria-specific (Figure 2). At the age of 5 wks, all four B6 mice were autoantibody-negative. By 12 wks of age, anti-nuclear and anti-nuclear rim reactive patterns appeared, with a concomitant reduction of anti-mitochondrial reactivity. The intensity of anti-nuclear reactivity was strong for three of the four Sap mice at 12 wks of age, with one showing weaker reactivity. For 12-wk old B6 mice, one showed weak nuclear reactivity with the remaining three showing no reactivity. At 24 wks of age, all four Sap mice, regardless of sex, showed very intense anti-nuclear reactivity. While two of the four control B6 mice at 24 wks of age had no reactivity, the other two had weak reactivity. Autoreactive antibodies appeared in Sap mice at a relatively young age and continued to increase in intensity in an age-dependent manner. Young B6 control mice were uniformly negative for autoantibodies, but as they age, weakly autoreactive antibodies also became apparent in

approximately half of the mice, a finding similar to the age-dependent increase in ANA-reactivity in healthy humans who are without disease symptoms (Xavier et al., 1995). Consistent with other studies (McMurray and May, 2003), ANA-reactivity is greater in females than males, possibly due to estrogen levels in females.

The development of serum autoantibodies in Sap mice was further confirmed by immunofluorescence staining of liver from IgH-KO mice (Figure 3). At 5 wks of age, all four Sap mice showed weak anti-nuclear and anti-cytoplasmic antibodies while none of the B6 control mice were autoantibody-positive. By 12 wks of age, strong nuclear staining patterns were observed in three out of the four Sap mice, with the remaining mouse showing weak nuclear staining. For B6 mice at 12 wks of age, one showed weak anti-cytoplasmic staining, another showed weak nuclear and cytoplasmic staining, and the others were autoantibody-negative. All Sap mice developed strong nuclear and cytoplasmic autoantibodies by 24 wks of age. Two of the four age-matched B6 mice showed weak nuclear and cytoplasmic reactivities similar to the level detected in 5-wk-old Sap mice. Therefore, the presence of autoantibodies in 5-wk old Sap mice and an age-dependent increase in autoantibodies were confirmed using IgH-KO liver sections as targets.

Immunocytochemical studies in one of the Sap female mice yielded five distinct liver-specific autoantibody staining patterns (Figure 4). In contrast to the three patterns

(nuclear, nuclear rim, and cytoplasmic) identified using B16-F10 target cells, nuclear, nucleolar-like, cytoplasmic punctate, cytoplasmic, and membranous patterns were identified when liver sections were stained. Located within the nucleus was the intense nucleolar-like staining which co-localized with the nuclear marker, Hoechst 33342, whereas a bright punctate staining was localized in the cytoplasm. Moreover, the membranous pattern was co-localized with the pancytokeratin staining. These three staining patterns were not observed in B16-F10 cells. Thus, autoreactive patterns appeared to be dependent on the target cells used and that both general as well as tissue- or cell-specific staining patterns were observed.

3.2 Assorted autoantibody reactivity in Sap sera as a function of age

Serum samples from four Sap and four control B6 mice were then examined for the presence of age-related autoantibody reactivity by western blot against electrophoretically separated IgH-KO liver lysates (Figure 5). Greater IgG response against reactivity to three to nine liver antigens was recognized by Sap sera. In general, different antigenic profiles were identified by sera from different Sap mice; the antigenic profiles were not simple, and showed varying degrees of complexity. Some of the reactivities that were detected at 5 wks of age would decrease in intensity or disappear by 12 wks of age, and then reappear at 24 wks of age; for example, the

reactivity against the 70 kD self-antigen in Sap M#1, and the 130 kD in Sap M#2. Such changing and dynamic patterns are consistent with an ever on-going autoantibody response; when one subsides, another one starts. A strong autoantibody reactivity against a 43 kD self-antigen in Sap M#1 demonstrated an age-correlated decrease in intensity. There was also an autoantibody reactivity that appeared or disappeared abruptly at certain ages; for example, reactivity against self-antigen at 120 kD appeared only on wk 24, and 54 kD reactivity disappeared by 12 wks of age in Sap M#2 serum sample. In addition to these observations, female Sap mice generally expressed stronger autoreactivity than their male counterparts. Together, at least five distinct reactivity patterns were detected: (1) from high to low or none, then re-appear; (2) from high to low; (3) appear abruptly; (4) disappear abruptly; and (5) appear at >20 wks. Overall, the number of autoantigens being recognized by Sap sera progressively increased as a function of age.

In B6 control mice, a low level of IgG reactive autoantibodies against an 80-kD self-antigen was observed in three of the four mice at 12 wks of age. Weak autoantibody reactivity against a 94 kD self-antigen was detected only for the 5-wk old B6 M#1. At 24 wks of age, M#1 and M#2 were found to contain weak reactivities against 2-3 antigens whereas the two female mice showed strong reactivity against multiple antigens.

3.3 Glomerular deposits of Ig developed at early age in Sap mice

Autoantibody generation and immune complex deposition are two hallmarks of systemic lupus erythematosus (Kotzin, 1996). Renal immune complex deposition was therefore assessed for kidney sections of Sap and B6 control mice (Figure 6). Deposits of immune complexes were identified in two (1M, 1F) of the four Sap mice as young as 5 to 6 wks of age. By 12 to 14 wks of age, immune complex deposition was detectable in all four Sap mice. Such deposits were not identified in B6 mice either at 5 to 6 wks or 12 to 14 wks of age. By 24-wk, all four Sap mice showed increased levels of immune complex deposition in their glomeruli. Extremely weak glomerular Ig deposits were also detectable in the two B6 mice at 24 wks of age. These findings are suggestive of an age-associated increase in immune complex deposition in Sap mice. In addition, H&E-stained renal sections showed larger glomeruli in Sap than B6 mice (Figure 7A & B); this enlargement in female but not male Sap mice was significantly different from B6 mice. The slightly enlarged Sap glomeruli are suggestive of inflammation, possibly dependent on IFN- γ , a potent activator of macrophages. Taken together, Sap mice meet the criteria for class I lupus nephritis defined as minimal mesangial lupus nephritis with mesangial immune deposits (Weening et al., 2004).

To further extend the potential targets of the Sap autoreactive antibodies to kidney antigens, sections made from IgH-KO kidneys were stained with serum samples

collected from four Sap mice (2M, 2F) and two B6 mice (1M, 1F) at 24 to 41 wks of age. Serum autoantibodies of the four Sap mice bound to nuclear antigens rather than glomerular antigens; B6 sera did not contain autoreactive antibodies (Figure 8). These results suggest that neither glomerular antigens nor circulating antigens localized within glomeruli are the target of Sap autoreactive antibodies, indicating that circulating immune complexes were deposited directly in the glomeruli of Sap mice.

3.4 Presence of predominant IgG2a, IgG1, but not IgM anti-nuclear autoantibody

Ig class switch is controlled by cytokines. While IL-4 promotes Th2 antibody response which is characterized by IgG1/IgE subclass production, IFN- γ promotes Th1 antibody response which is characterized by IgG2a antibody production. It is therefore of interest to determine the ANA subclass distribution. Representative mouse serum samples collected from Sap (2M, 2F) and B6 (1M, 1F) mice at 24 wks of age were used to stain B16-F10 cells, followed by detection of cell-bound autoantibodies by subclass-specific antibodies. The results demonstrated that IgM autoantibodies were undetectable in all Sap and B6 mice. The autoantibodies in three of the four Sap mice were mainly of the IgG2a isotype, but their intensities varied (Figure 9). Sap F#2 contained extremely weak, IgG2a autoantibodies. One of the female Sap mice produced had strong IgG2a autoantibodies but weak IgG1 autoantibodies. As other

isotype-specific antibodies were not examined, the autoantibodies in Sap M#2 and F#2 might belong to subclasses other than IgG1, IgG2a, and IgM. As expected, none of the B6 control mice showed detectable autoreactivity. These results indicate that IgG2a constituted the most dominant ANA response, although weaker IgG1 ANA response could happen also. Altogether, the main pathway leading to autoantibody production in Sap mice is mediated through Th1 cells.

3.5 Renal immune complex deposits were mostly IgM type

Based on the finding that IgG2a but not IgM was found to be the major autoantibody subclass in Sap mouse serum, it seems that IgG2a but not IgM is more likely to be involved in the formation of immune complex that is then trapped in the kidney. To address this possibility, immune complexes deposited in the kidneys from Sap (2M, 2F) and B6 (1M, 1F) mice at age ranging from 24-41 wks were examined for isotype distribution. Strong IgM presence in kidney glomeruli was observed in kidney sections of all four examined Sap mice. Weak IgG1 and IgG2a immune complex deposits were found in both female Sap mice. For the two male Sap mice, no IgG1 was detected, although weak IgG2a was detected in one mouse (Figure 10). For control B6 mice, the male mouse developed negligible immune complex deposition whereas the female mouse contained only IgM deposits.

3.6 CD4⁺ T cells are required for germinal center reaction in Sap mice

Affinity maturation inside the germinal center results in the selection of B cells which secrete high affinity antibodies. The presence of high-titered autoantibodies in Sap mice is likely the result of significant on-going germinal center reactions. GL7 antibody was used to detect GC as GC B cell blasts express high amounts of the GL7 epitope (Kelsoe, 1996). The number of GCs in Sap spleen was 3-fold higher than that found in B6 spleen (Figure 11C). It has long been established that CD4⁺ T helper cells are the main player that initiates T-B cell interaction at the follicular border and subsequently, the GC formation (Goodnow et al., 2010). We studied the likely disruptive effect of CD4⁺ T cell depletion on GC formation in Sap mice. Sap mice were injected intravenously with 200 µg anti-CD4 mAb once on d0, and spleens were harvested on d2, d4, d7, and d10. By day 4 post-GK1.5 treatment, GCs significantly decreased in number and size (Figure 11C). Upon the re-appearance of CD4⁺ T cells, GCs re-formed. On d10 after the anti-CD4 mAb treatment, the number and size of GCs had returned to the original level, indicating that the newly formed CD4⁺ T cells contained significant numbers of autoreactive cells. CD4⁺ T cell presence and GCs were assayed by immunofluorescence staining. On spleen frozen sections taken from anti-CD4-treated mice, no CD4⁺ T cells were detectable on d2 and d4, and became visible on d7 (Figure 11A). Flow cytometry analysis also confirmed that anti-CD4 mAb treatment resulted in

complete depletion of CD4⁺ T cells 2 to 4 days post-treatment (Figure 11B), with repopulation of CD4⁺ T cells starting to take place after d4.

Given the role of CD4⁺ T cells in GC formation, 2 doses of 200 µg anti-CD4 mAb, one at d0 and the other at d4, were administered intravenously to a Sap mouse (Figure 12A) to further confirm that the GC reaction is solely dependent on CD4⁺ T cells. Spleen was harvested from the mouse 5 days after anti-CD4 mAb treatment. No GCs were found in the spleen of the mouse using immunofluorescence staining of spleen frozen sections (Figure 12B & C). Thus, a longer duration without CD4⁺ T cells can completely abolish the GC reaction. Together, these data showed that CD4⁺ T cells in Sap mice contain significant numbers of autoreactive cells. The autoreactive CD4⁺ T cells help B cells to initiate greater GC reaction in Sap mice spontaneously without intentional immunization.

We also generated Sap-CD4-KO mice to study the effect of lacking CD4⁺ T cells on the formation of autoantibody and GC. Spleens were harvested from Sap (M), Sap-CD4-KO (1M, 2F), CD4-KO (1M, 1F), and B6 (M) mice at 12 to 14 wks of age. Surprisingly, GCs were found in Sap mice in the absence of CD4⁺ T cells (Figure 13 B), indicating cells other than CD4⁺ T cells can help B cells from GCs. The size of GCs was significantly reduced and the number of GCs varied (Figure 13 C). One Sap-CD4-KO mouse developed weak autoantibodies and a high number of GCs in spleen (Figure 13A

& C).

3.7 IFN- γ -dependency of autoantibody response in Sap mice

It has been reported that IFN- γ promotes IgG2a isotype switch and production by directly acting on B cells (Kalinski and Moser, 2005). Based on this, the role of IFN- γ in autoantibody response was examined. Since Sap mice contained mostly IgG2a serum autoantibodies (Figure 9), the autoantibody response might be driven by IFN- γ . Immunofluorescence staining of serum samples from one Sap, four Sap-IFN- γ -KO, and one B6 mice collected at 12 to 14 wks of age using fixed B16-F10 target cells demonstrated that the four Sap-IFN- γ -KO mice developed weak anti-cytoplasmic autoantibodies (ACA) but not ANA (Figure 14A). The B6 control was autoantibody-negative whereas the Sap control showed abundant ANA. In addition, in the absence of IFN- γ , the Sap-IFN- γ -KO mice still showed significant number of GCs in the spleen comparable to Sap mice, although significant variations in the size of GCs were observed (Figure 14B & C). These data suggested that the generation of IgG2a ANA in Sap mice indeed requires stimulation from cytokine IFN- γ on Sap B cells.

3.8 Reduced Ig deposits in the absence of IFN- γ

IFN- γ has been reported to contribute to ANA production and to strengthen the

severity of glomerulonephritis (GN) in several studies (Balomenos et al., 1998; Haas et al., 1998). To evaluate the effect of IFN- γ on the deposits of Ig in Sap kidney, the renal immune complex deposition was identified in one Sap (F) mice, four Sap-IFN- γ -KO (2M, 2F) mice, and one B6 (F) mice at 12 to 14 wks of age. Consistent with previously published findings, immune complex deposits were greatly diminished in the glomeruli of three of the four Sap-IFN- γ -KO mice (Figure 15). Sap-IFN- γ -KO M#2 mouse exhibited reduced yet detectable immune complex deposits. These results indicate that the formation of immune complexes is IFN- γ -dependent.

3.9 Predominance of IgG1 and IgG2b subclasses of anti-cytoplasmic autoantibodies in Sap-IFN- γ -KO mice

The Ig subclass of the ACA observed for Sap-IFN- γ -KO mice was next studied. Serum from a Sap-IFN- γ -KO (F) mouse (23 wks of age) was applied to B16-F10 target cells, followed by detection of cell-bound autoantibodies by isotype-specific antibodies. Strong IgG1 and IgG2b ACA, together with relatively weak IgG2a and IgG3 ACA were detected (Figure 16). The presence of weak IgG2a ACA in Sap-IFN- γ -KO suggests that although IFN- γ can drive IgG2a ANA production, it is not exclusively required.

3.10 Sap CD4⁺ T cells can reconstitute anti-nuclear autoantibody response in

Sap-CD4-KO mice but not in Sap-IFN- γ -KO

Relatively weak ANA reactivity in young Sap mice raised the following issue about whether these low autoreactive CD4⁺ T cells from young Sap mice could induce autoantibody response in older Sap mice. Sort-purified CD4⁺CD25⁻ T cells (10⁷ cells) from 4-wk old Sap or B6 mice were sorted and adoptively transferred into two 12-wk old Sap-CD4-KO mice, respectively (Figure 17A). At 4 wks of age, Sap mice had not developed strong ANA. Peripheral blood was collected from the recipients on d-1, d7, d14, and d21 to monitor the presence of donor CD4⁺ T cells. Serum samples were tested for ANA using B16-F10 target cells. On d7 days following Sap CD4⁺ T cell transfer, ANA was detected in Sap-CD4-KO host mice; the ANA reactivity was maintained up to 21d post-CD4⁺ T cell transfer (Figure 17C). The number of Sap CD4⁺ donor T cells progressively increased, whereas B6 CD4⁺ T cells progressively decreased over time (Figure 17B). The environment required for Sap CD4⁺ T cells may be different from that for B6 CD4⁺ T cells. Alternatively, significant expansion of autoreactive Sap CD4⁺ T cells took place after they were adoptively transferred into Sap-CD4-KO hosts. In addition, this result indicates that autoreactive CD4⁺ T cells are present in young Sap mice and the failure of these mice to make ANA is likely due to an active suppression mechanism that prevents autoreactive CD4⁺ T cells from providing help in antibody affinity maturation.

If CD4⁺ T cells are the source of IFN- γ that is required for IgG2a antibody isotype switch and affinity maturation, transferring Sap CD4⁺ T cells into Sap-IFN- γ -KO mice should induce ANA production. Total spleen cells (8×10^7 cells) and CD4⁺CD25⁻ T cells (8.5×10^6 cells) obtained from Sap mice were adoptively transferred to one Sap-IFN- γ -KO mouse and two Sap-IFN- γ -KO mice, respectively (Figure 18A). Control Sap-IFN- γ -KO mice received no transferred cells. Serum samples collected on d-1, d7, d14, d21 post-transfer were examined for autoantibody against B16-F10 target cells. Surprisingly, no ANA was detected in any of the recipient mice (Figure 18B). Even though Sap-IFN- γ -KO recipients did not produce ANA, they nevertheless made ACA, indicating a positive correlation between IFN- γ and ANA response. The result suggests that Sap CD4⁺ T cells are not the source of IFN- γ required for ANA formation. Moreover, it is more difficult to explain the failure of transferred total Sap spleen cells to reconstitute ANA response in the Sap-IFN- γ -KO host mice. A technical concern of incompatibility between donor Sap spleen cells and host Sap-IFN- γ -KO hosts needs to be ruled out first.

3.11 Autoantibody response in Sap mice is partially dependent on NKT cells but not CD8⁺ T cells

Serum samples were collected from Sap (M), Sap-CD8-KO (2F), CD8-KO (1M,

1F), Sap-CD1d-KO (2M, 2F), CD1d-KO (1M, 1F), and B6 (M) mice at age ranging from 12-14 wks, and examined for autoreactivity against B16-F10 target cells. Sap mice deficient in CD8⁺ T cells developed autoantibodies with very strong nuclear rim reactivity, clearly detectable but weaker nuclear reactivity, and still yet weaker anti-cytoplasmic reactivity (Figure 19). One of the CD8-KO mice contained detectable ANA. In addition, CD1d deficient mice lack of CD1d-expression on antigen presenting cells and CD1d-activated NKT cells (Exley et al., 2003). Screening results revealed that Sap mice deficient in NKT cells displayed intermediate level of anti-nuclear, anti-nuclear rim, and anti-cytoplasmic reactivity. None of the CD1d-KO control mice developed autoantibodies. Based on the observed requirement of IFN- γ for the generation of ANA, the results ruled out the possibilities of CD8⁺ T cells being the IFN- γ producing cells and the involvement of CD8⁺ Tregs. These data imply a role for NKT cells in the generation of ANA through IFN- γ production.

To understand the importance of $\alpha\beta$ T cells in helping autoantibody production, and how depletion of MHC class II might affect production of autoantibodies, Sap mice deficient in $\alpha\beta$ T cells or MHC class II molecules were generated. Serum autoantibodies were analyzed in Sap-TCR β -KO (2M2F), TCR β -KO (1M1F), Sap-KOII (2M1F), and KOII (1M1F) mice by IF staining against B16-F10 target cells. Two of the four Sap-TCR β -KO mice developed relatively weak ANA and ACA (Figure 20), which

indicates that cells other than TCR- $\alpha\beta$ cells are able to help autoantibody production.

Sap-KOII mice did not generate any detectable autoantibodies as expected.

Autoantibodies were absent in the control mice, TCR β -KO and MHC-II-KO mice.

Spleen frozen sections of Sap-CD8-KO, Sap-CD1d-KO, and Sap-TCR β -KO mice were stained with A488-Thy1.2, A546-B220, and A647-GL7. Quantification of GCs in the spleens revealed that TCR β chain-deficient mice developed significantly smaller and fewer GCs. GC size and number in Sap-CD8-KO mice were similar to Sap mice. GC size was scientifically reduced in Sap-CD1d-KO mice (Figure 21), which was consistent with the observation that Sap-CD1d-KO mice generated lower-titered autoantibodies (Figure 19). Together the results indicate that ANA production is highly dependent on TCR- $\alpha\beta$ cells.

Discussion

4.1 Characterization of autoantibody production in Sap mice

Sap is an ENU-induced mutant mouse strain with a point mutation in the *Zap70* gene. The studies presented here are designed to characterize as well as gain mechanistic understanding the autoantibody response in Sap mice. The 3- to 4-fold reduction in *Zap70* protein expression, combined with a ~10-fold reduced intrinsic kinase activity caused reduced CD4⁺ T cell development and failure to delete autoreactive T cells (F.-L. Chen & Y.-T. Chen, unpublished results).

I have generated results that clearly demonstrate that the autoantibody response in Sap mice requires MHC-II-restricted CD4⁺ T cells and IFN- γ . Autoreactive T cells that recognize self antigens presented by antigen-presenting cells are required to initiate autoantibody response. Activated autoantigen-specific B cells proliferate and migrate into GC where they interact with T_{FH} and follicular dendritic cells (FDC), undergo class switch recombination and affinity maturation, and finally differentiate into plasma cells that produce autoantibodies (Goodnow et al., 2010). Autoantibody response does not take place when any of these elements is missing. In this study, IF staining of serum autoantibodies and splenic GCs from Sap mice made deficient in CD4, CD8, CD1d, TCR β , and MHC-II either by mAb treatment or by genetic ablation were studied. Treatment of Sap mice with anti-CD4 mAb resulted in complete elimination of all GCs

(Figure 12), clearly indicating the critical dependence of GC formation on CD4⁺ T cells. Thus, one might expect highly deficient formation of GCs in Sap mice on a CD4-KO genetic background. However, GCs were found in Sap-CD4-KO mice in the absence of strong autoantibodies (Figure 13). CD4 coreceptor-independent, MHC class II-restricted CD4⁻CD8⁻TCRαβ⁺ T cells have been shown to mediate GC formation in CD4-KO mice (Locksley et al., 1993). If this conclusion is applicable to autoantibody generation in Sap mice, then no GC formation is expected when all TCR-αβ T cells are eliminated. Indeed, scanty and weak GC formation was seen in Sap-TCRβ-KO mice (Figure 20). Despite the highly significant reduction in the magnitude of autoantibody in Sap-TCRβ-KO mice, weak autoantibody was nevertheless detected. TCR-γδ cells may play a role in the initiation of this weak autoantibody response as they have been reported to act as helper cells to induce anti-DNA autoantibodies (Rajagopalan et al., 1990). Thus, even though MHC-II-restricted CD4⁺ helper T cells play a dominant role in helping autoantibody response, weak autoantibody response and GC reaction can take place in the absence of CD4⁺ T cells. CD8⁺ T cells are precursors of cytolytic effectors, and antibody response is unaffected by their absence. Consistent with this, the formation of autoantibodies and GCs in Sap mice was not affected by genetic ablation of CD8⁺ T cells (Figure 19). In contrast to (NZB × NZW)F1 (BWF1) mice in which CD1d deficiency exacerbates autoantibody formation (Yang et al., 2007), CD1d

deficiency in Sap mice caused a partial decrease in the ANA response, possibly due to the loss of IFN- γ secreted by NKT cells. As Sap-KOII mice have just recently become available, only ANA response analysis has been completed. ANA was undetectable in two of the three Sap-KOII-KO mice, with a very weak response detected in the third mouse.

Although ANA and ACA were both produced in Sap mice, they were not generally produced at the same time; younger Sap mice make mostly ACA and older Sap mice produce exclusively ANA (Figure 1). At this point, it is unclear why and how they undergo this transition. Since IFN- γ is critically required for ANA production, an age-associated increase in IFN- γ production, possibly by NK cells, may be the trigger for the ACA to ANA switch response. It should be noted that the mechanism by which IFN- γ promotes ANA response is far from clear, but its known effect on IgG2a isotype switch as well as its effect on increased antigen processing and presentation can be two interesting areas for future investigation.

Sap-CD4-KO mice were characterized by poor ANA response. Adoptive transfer of Sap CD4⁺ T cells taken from 4-wk old mice into 12-wk old Sap-CD4-KO mice restored the ANA response (Figure 17). From this result, we can infer that autoreactive CD4⁺ T cells are present in 4-wk old Sap mice. Why then is ANA response not observed in 4-wk old Sap mice? It may be that the number of autoreactive CD4⁺ T cells is too few in 4-wk

old Sap mice to initiate an ANA response. This seems unlikely as autoreactive CD4⁺ T cells can undergo rapid clonal expansion when they engage properly presented autoantigen. It is possible that the efficiency for autoantigen processing and presentation by dendritic cells (DC) increases in older Sap mice either due to increased availability of nuclear antigens caused by increased cell damage or by increased factors (e.g., IFN- γ) that promote antigen processing/presentation. The older Sap mice contain more B cells that are autoreactive against nuclear antigens, although this possibility had found no support from the published literature.

Intriguingly, when Sap spleen cells or purified CD4⁺CD25⁻ T cells were transferred into the ANA response-deficient Sap-IFN- γ -KO mice, restoration of ANA failed (Figure 18). Recent data showed that DC derived from IFN- γ -KO mice had enhanced antigen presentation and IL-12 secretion (Wu et al., 2006), implying that deficiency in IFN- γ likely has an impact on necessary components other than DC for a successful autoantibody production. Further studies are required to clarify the mechanism of IFN- γ on antigen presentation in Sap mice. One potential way to investigate this issue may be to use OVA-pulsed CD11c⁺ splenic DC derived from Sap-OTII and Sap-IFN- γ -KO-OTII mice in co-cultures with responder T cells derived from Sap-OTII mice. Using this model, one can assess the extent of T cell proliferation as an indirect measure of the efficiency of DC at activating T cells. Given that the total

spleen cells from Sap donor mice contain IFN- γ -producing cells, the problem should lie within the Sap-IFN- γ -KO host. It is possible that the autoimmune-prone microenvironment in Sap mice favoring the survival of autoreactive Sap CD4⁺ T cells does not promise a good survival of transferred Sap cells in an IFN- γ deficient microenvironment. However, T cell survival in general is not affected by the absence of IFN- γ . Should IFN- γ play a role in the survival of autoreactive CD4⁺ T cells, then its mechanism must be significantly unique to autoreactive T cells and not T cells in general. Whether Sap CD4⁺ T cells indeed survive poorly in an IFN- γ -deficient host environment can be addressed by adoptive transfer of CD4⁺ T cells taken from Sap-eGFP tg mice, followed by flow cytometric analysis of GFP⁺ donor cells.

4.2 Non-CD4⁺ T cell source of IFN- γ in autoantibody production

IFN- γ is a pleiotropic cytokine that has been shown to be involved in regulating autoimmune diseases. It is also known to influence IgG2a class switch (Reinhardt et al., 2009). The generation of IgG2a ANA in Sap mice was clearly IFN- γ -dependent (Figure 14). In the absence of IFN- γ , IgG2a ANA was lost and IgM immune complex deposition in the kidney was reduced, suggesting an IFN- γ role in both IgG2a and IgM autoantibody production (Figure 14 & 15). This result is consistent with the Lyn-deficient autoimmune mouse model in which IFN- γ deficiency reduces IgG2a

anti-DNA antibody and IgM immune complexes (Scapini et al., 2010). Recently, it has been reported that IL-17 and IL-21 promote class switch to IgG2a/IgG3, and IgG1/IgG2b, respectively (Mitsdoerffer et al., 2010). Therefore, class switch to IgG2a can take place in the absence of IFN- γ even though IFN- γ is a dominant factor that drives IgG2a isotype switch.

The fact that depletion of IFN- γ resulted in complete loss of high-affinity IgG2a autoantibodies without affecting GC formation (Figure 14 B & C) implies that IFN- γ may not affect binding affinity of nuclear antigens in the priming phase yet is required to induce class switch to IgG2a. In the absence of IFN- γ , it is likely that GC B cells can only undergo class switch to immunoglobulin class other than IgG2a. As T_{FH} cells express the class switch factor IFN- γ that enhances the production of IgG2a antibodies directly and locally in GC (Reinhardt et al., 2009), it will be of interest to determine whether high affinity IgG2a ANA would still arise in situations where T_{FH} cells do not produce IFN- γ .

NK cells and $\gamma\delta$ T cells are considered to be the first line of defense in innate immunity against bacterial infections (Kaufmann, 1996; Lunemann et al., 2009). NK cells are known to be potent IFN- γ producers. Upon activation by antigen-primed DC directly or by cytokine signals such as IL-18 and IL-12 indirectly, NK cells secrete a large amount of IFN- γ (Borg et al., 2004; Orange and Biron, 1996). IL-12 and IL-18 are

produced by DC and macrophages in response to pathogenic stimuli (Szabo et al., 2003).

It is therefore worthwhile to examine whether there is elevated IL-12 and IL-18 production in Sap mice. The finding of elevated IL-18 in autoimmune inflammatory myopathies may be relevant in this context (Tucci et al., 2006). Previous studies have shown that activated NK cells can direct B cells toward IgG2a isotype switch (Gao et al., 2001; Gao et al., 2008). Thus, the finding of high-titered IgG2a autoantibodies in older Sap mice may be caused by high IFN- γ production by NK cells in older but not younger Sap mice. Depletion of NK cells using anti-asialo-GM1 (ASGM) should provide additional clues to the role of NK cells in IgG2a ANA response in Sap mice. Another possible approach would be to breed Sap onto the NK cell-deficient Il-15-KO background (Kennedy et al., 2000). It is of interest to study whether ANA can be restored in Sap-IFN- γ -KO hosts adoptively transferred with Sap NK cells with or without Sap CD4⁺ T cells. Another interesting experiment is to transfer CD4⁺ T cells from Sap-IFN- γ -KO mice into Sap-CD4-KO hosts and observe for restoration of ANA response. If ANA can be restored, then source of IFN- γ must not be a CD4⁺ T cell. If ANA is not restored, it may mean CD4⁺ T cells are mostly devoid of autoreactive specificities, and that IFN- γ presence positively impacts on the development, expansion, or maintenance of autoreactive CD4⁺ T cells.

4.3 Autophagy and ANA response

Macroautophagy is a constitutively active process in eukaryotic cells. In macroautophagy, intracellular components and long-lived proteins are delivered via a double-membrane autophagosome to endosomes for lysosomal degradation (Crotzer and Blum, 2010). Degraded antigenic fragments are loaded onto the MHC-II molecules in the MHC-II-containing compartment (MIIC). The observation that only some but not all CD4⁺ T cells are positively selected in the absence of autophagy in Atg5-deficient mice, in combination with the finding that constitutive macroautophagy is detected in thymic epithelial cells (TEC) (Nedjic et al., 2008), confirm that macroautophagy in TEC is intimately involved in thymic positive selection. It has been reported that treating macrophages with IFN- γ upregulates autophagy (Singh et al., 2006). Other than that, little has been mentioned about IFN- γ and its role in macroautophagy or thymic positive selection. How IFN- γ mediates its effect on autoantibody production and nuclear antigen presentation is still not known at this time. It is worthwhile to compare total thymic IFN- γ mRNA between B6 and Sap mice, and between 3-wk old and 8-wk old Sap mice. If no differences in total IFN- γ mRNA is found, then it is unlikely that the IFN- γ -dependence reported here is mediated through its effect on thymic positive selection.

4.4 Immune complex deposition in Sap kidney without glomerulonephritis

Sap mice displayed enlarged glomeruli and Ig deposits, two histological features of acute glomerulonephritis (Yu et al.) (Figure 7). However, in Sap mice, deposition of immune complexes did not give rise to tissue damage, similar to B6.NZMc1 mice that are congenic for the NZM2410-derived *Sle1* interval, a locus on chromosome 1 that has been thought to be linked with autoimmune glomerulonephritis (GN) (Mohan et al., 1999). B6.NZMc1 mice are free of GN and only contain anti-H2A, -H2b, -DNA ANA. In contrast, NZM.C57Lc4 mice in which the autoantibody contributing genetic interval on chromosome 4 is replaced by corresponding interval from nonlupus-prone C57/L mice develop serious immune complexes and GN but are free of anti-dsDNA and anti-nuclear autoantibodies (Waters et al., 2004). These findings show that ds-DNA or anti-nuclear autoantibodies are not necessarily a prerequisite for GN development.

Three theories for the formation of immune complex that lead to lupus nephritis have been proposed: (A) circulating antibody-antigen immune complexes deposit directly in glomeruli, (B) autoantibodies bind directly to glomerular antigens, and (C) binding of autoantibodies to antigens that have already been trapped within glomeruli (Waldman and Madaio, 2005; Weening et al., 2004). The possibility that Sap serum autoantibodies contain specific binding affinity to glomerular antigens was ruled out because Sap autoantibodies reacted only with nuclear antigens and nothing else in the

glomerulus (Figure 8). Several studies have demonstrated that the pathogenicity of autoantibodies depends on their immunoglobulin subclass and ability to deposit in the glomeruli (Madaio et al., 1987; Pankewycz et al., 1987). My finding that the majority of immune complexes deposited in the Sap glomeruli are composed of IgM:Ag (Figure 10) suggests that the IgG2a-dominant ANA do not form immune complexes efficiently and that autoreactive IgM autoantibodies form immune complexes efficiently; they do not recognize antigens associated with cell-associated antigens and may recognize secreted soluble proteins. My finding of IgM immune complexes in the kidney without serious pathology is consistent with the report that IgM autoantibody is not as pathogenic as IgG autoantibody (Korganow et al., 1999).

To fully address acute glomerulonephritis, additional histological abnormalities and clinical features should be considered. Enlarged glomeruli are signs of cell proliferation within the glomerular or neutrophilic infiltration. Obvious hypercellularity was not observed within Sap glomeruli, suggesting that neither neutrophils nor macrophages were activated (Figure 7). IFN- γ is known to contribute to the severity of glomerulonephritis and the amount of Ig and C3 complement deposited in BWF1 mice (Haas et al., 1998). Consistent with the diminished immune complex deposition detected in Sap mice lacking IFN- γ (Figure 15), BW mice deficient in IFN- γ R (Haas et al., 1998), MRL/lpr mice deficient in IFN- γ (Balomenos et al., 1998), or treatment with

soluble IFN- γ R or anti-IFN- γ mAb to MRL/lpr mice for up to 12 wks (Ozmen et al., 1995) decrease the deposition of Ig and reduce the severity of GN. Also, MHC class II upregulation in the renal proximal tubules has been reported to be responsible for the nephritis in MRL/lpr mice through the local presentation of autoantigens to T cells and trigger inflammatory immune response (Wuthrich et al., 1989). It is possible that IFN- γ level in Sap kidney is below the threshold for disease progression and MHC class II upregulation. One can evaluate the level of MHC class II expression in the renal proximal tubules. However, exactly how IFN- γ influences autoantibodies production and GN is still unclear. Future research can focus on the many possible mechanisms of how IFN- γ contributes to immune complex deposition and pathological kidney function. Whether IFN- γ plays a role in the IgM autoantibody response should be clarified first.

References

Au-Yeung, B.B., Deindl, S., Hsu, L.Y., Palacios, E.H., Levin, S.E., Kuriyan, J., and Weiss, A. (2009). The structure, regulation, and function of ZAP-70. *Immunol Rev* 228, 41-57.

Balomenos, D., Rumold, R., and Theofilopoulos, A.N. (1998). Interferon-gamma is required for lupus-like disease and lymphoaccumulation in MRL-lpr mice. *J Clin Invest* 101, 364-371.

Benson, G.D., Kikuchi, K., Miyakawa, H., Tanaka, A., Watnik, M.R., and Gershwin, M.E. (2004). Serial analysis of antimitochondrial antibody in patients with primary biliary cirrhosis. *Clinical & developmental immunology* 11, 129-133.

Bertry-Coussot, L., Lucas, B., Danel, C., Halbwachs-Mecarelli, L., Bach, J.F., Chatenoud, L., and Lemarchand, P. (2002). Long-term reversal of established autoimmunity upon transient blockade of the LFA-1/intercellular adhesion molecule-1 pathway. *J Immunol* 168, 3641-3648.

Borg, C., Jalil, A., Laderach, D., Maruyama, K., Wakasugi, H., Charrier, S., Ryffel, B., Cambi, A., Figdor, C., Vainchenker, W., *et al.* (2004). NK cell activation by dendritic cells (DCs) requires the formation of a synapse leading to IL-12 polarization in DCs. *Blood* 104, 3267-3275.

Crotzer, V.L., and Blum, J.S. (2010). Autophagy and adaptive immunity. *Immunology* 131, 9-17.

Eriksson, C., Kokkonen, H., Johansson, M., Hallmans, G., Wadell, G., and Rantapaa-Dahlqvist, S. (2011). Autoantibodies predate the onset of systemic lupus erythematosus in northern Sweden. *Arthritis research & therapy* 13, R30.

Exley, M.A., Bigley, N.J., Cheng, O., Shaulov, A., Tahir, S.M., Carter, Q.L., Garcia, J., Wang, C., Patten, K., Stills, H.F., *et al.* (2003). Innate immune response to encephalomyocarditis virus infection mediated by CD1d. *Immunology* 110, 519-526.

Gao, N., Dang, T., and Yuan, D. (2001). IFN-gamma-dependent and -independent initiation of switch recombination by NK cells. *J Immunol* 167, 2011-2018.

Gao, N., Jennings, P., and Yuan, D. (2008). Requirements for the natural killer cell-mediated induction of IgG1 and IgG2a expression in B lymphocytes. *Int Immunol* 20, 645-657.

Gershwin, M.E., Coppel, R.L., and Mackay, I.R. (1988). Primary biliary cirrhosis and mitochondrial autoantigens--insights from molecular biology. *Hepatology* 8, 147-151.

Goodnow, C.C., Vinuesa, C.G., Randall, K.L., Mackay, F., and Brink, R. (2010). Control systems and decision making for antibody production. *Nat Immunol* 11, 681-688.

Haas, C., Ryffel, B., and Le Hir, M. (1998). IFN-gamma receptor deletion prevents autoantibody production and glomerulonephritis in lupus-prone (NZB x NZW)F1 mice. *J Immunol* 160, 3713-3718.

Hemmelgarn, B.R., Manns, B.J., Lloyd, A., James, M.T., Klarenbach, S., Quinn, R.R.,

Wiebe, N., and Tonelli, M. (2010). Relation between kidney function, proteinuria, and adverse outcomes. *JAMA* 303, 423-429.

Hsu, L.Y., Tan, Y.X., Xiao, Z., Malissen, M., and Weiss, A. (2009). A hypomorphic allele of ZAP-70 reveals a distinct thymic threshold for autoimmune disease versus autoimmune reactivity. *J Exp Med* 206, 2527-2541.

Jakob, T., Kollisch, G.V., Howaldt, M., Bewersdorff, M., Rathkolb, B., Muller, M.L., Sandholzer, N., Nitschke, L., Schiemann, M., Mempel, M., *et al.* (2008). Novel mouse mutants with primary cellular immunodeficiencies generated by genome-wide mutagenesis. *J Allergy Clin Immunol* 121, 179-184 e177.

Kalinski, P., and Moser, M. (2005). Consensual immunity: success-driven development of T-helper-1 and T-helper-2 responses. *Nat Rev Immunol* 5, 251-260.

Kaufmann, S.H. (1996). gamma/delta and other unconventional T lymphocytes: what do they see and what do they do? *Proc Natl Acad Sci U S A* 93, 2272-2279.

Kelsoe, G. (1996). Life and death in germinal centers (redux). *Immunity* 4, 107-111.

Kennedy, M.K., Glaccum, M., Brown, S.N., Butz, E.A., Viney, J.L., Embers, M., Matsuki, N., Charrier, K., Sedger, L., Willis, C.R., *et al.* (2000). Reversible defects in natural killer and memory CD8 T cell lineages in interleukin 15-deficient mice. *J Exp Med* 191, 771-780.

Korganow, A.S., Ji, H., Mangialaio, S., Duchatelle, V., Pelanda, R., Martin, T., Degott,

C., Kikutani, H., Rajewsky, K., Pasquali, J.L., *et al.* (1999). From systemic T cell self-reactivity to organ-specific autoimmune disease via immunoglobulins. *Immunity* 10, 451-461.

Kotzin, B.L. (1996). Systemic lupus erythematosus. *Cell* 85, 303-306.

Linterman, M.A., Rigby, R.J., Wong, R.K., Yu, D., Brink, R., Cannons, J.L., Schwartzberg, P.L., Cook, M.C., Walters, G.D., and Vinuesa, C.G. (2009). Follicular helper T cells are required for systemic autoimmunity. *J Exp Med* 206, 561-576.

Locksley, R.M., Reiner, S.L., Hatam, F., Littman, D.R., and Killeen, N. (1993). Helper T cells without CD4: control of leishmaniasis in CD4-deficient mice. *Science* 261, 1448-1451.

Lunemann, A., Lunemann, J.D., and Munz, C. (2009). Regulatory NK-cell functions in inflammation and autoimmunity. *Mol Med* 15, 352-358.

Luzina, I.G., Atamas, S.P., Storrer, C.E., daSilva, L.C., Kelsoe, G., Papadimitriou, J.C., and Handwerker, B.S. (2001). Spontaneous formation of germinal centers in autoimmune mice. *J Leukoc Biol* 70, 578-584.

Mackay, I.R. (1958). Primary biliary cirrhosis showing a high titer of autoantibody; report of a case. *N Engl J Med* 258, 185-188.

Madaio, M.P., Carlson, J., Cataldo, J., Ucci, A., Migliorini, P., and Pankewycz, O. (1987). Murine monoclonal anti-DNA antibodies bind directly to glomerular antigens

and form immune deposits. *J Immunol* 138, 2883-2889.

Mattalia, A., Quaranta, S., Leung, P.S., Bauducci, M., Van de Water, J., Calvo, P.L., Danielle, F., Rizzetto, M., Ansari, A., Coppel, R.L., *et al.* (1998). Characterization of antimitochondrial antibodies in health adults. *Hepatology* 27, 656-661.

McMurray, R.W., and May, W. (2003). Sex hormones and systemic lupus erythematosus: review and meta-analysis. *Arthritis Rheum* 48, 2100-2110.

Mitsdoerffer, M., Lee, Y., Jager, A., Kim, H.J., Korn, T., Kolls, J.K., Cantor, H., Bettelli, E., and Kuchroo, V.K. (2010). Proinflammatory T helper type 17 cells are effective B-cell helpers. *Proc Natl Acad Sci U S A* 107, 14292-14297.

Miyakawa, H., Tanaka, A., Kikuchi, K., Matsushita, M., Kitazawa, E., Kawaguchi, N., Fujikawa, H., and Gershwin, M.E. (2001). Detection of antimitochondrial autoantibodies in immunofluorescent AMA-negative patients with primary biliary cirrhosis using recombinant autoantigens. *Hepatology* 34, 243-248.

Mohan, C., Morel, L., Yang, P., Watanabe, H., Croker, B., Gilkeson, G., and Wakeland, E.K. (1999). Genetic dissection of lupus pathogenesis: a recipe for nephrophilic autoantibodies. *J Clin Invest* 103, 1685-1695.

Nedjic, J., Aichinger, M., Emmerich, J., Mizushima, N., and Klein, L. (2008). Autophagy in thymic epithelium shapes the T-cell repertoire and is essential for tolerance. *Nature* 455, 396-400.

Nurieva, R.I., Chung, Y., Martinez, G.J., Yang, X.O., Tanaka, S., Matskevitch, T.D., Wang, Y.H., and Dong, C. (2009). Bcl6 mediates the development of T follicular helper cells. *Science* 325, 1001-1005.

Orange, J.S., and Biron, C.A. (1996). An absolute and restricted requirement for IL-12 in natural killer cell IFN-gamma production and antiviral defense. Studies of natural killer and T cell responses in contrasting viral infections. *J Immunol* 156, 1138-1142.

Ozmen, L., Roman, D., Fountoulakis, M., Schmid, G., Ryffel, B., and Garotta, G. (1995). Experimental therapy of systemic lupus erythematosus: the treatment of NZB/W mice with mouse soluble interferon-gamma receptor inhibits the onset of glomerulonephritis. *Eur J Immunol* 25, 6-12.

Pankewycz, O.G., Migliorini, P., and Madaio, M.P. (1987). Polyreactive autoantibodies are nephritogenic in murine lupus nephritis. *J Immunol* 139, 3287-3294.

Rajagopalan, S., Zordan, T., Tsokos, G.C., and Datta, S.K. (1990). Pathogenic anti-DNA autoantibody-inducing T helper cell lines from patients with active lupus nephritis: isolation of CD4-8- T helper cell lines that express the gamma delta T-cell antigen receptor. *Proc Natl Acad Sci U S A* 87, 7020-7024.

Reinhardt, R.L., Liang, H.E., and Locksley, R.M. (2009). Cytokine-secreting follicular T cells shape the antibody repertoire. *Nat Immunol* 10, 385-393.

Sakaguchi, N., Takahashi, T., Hata, H., Nomura, T., Tagami, T., Yamazaki, S., Sakihama, T., Matsutani, T., Negishi, I., Nakatsuru, S., and Sakaguchi, S. (2003). Altered thymic

T-cell selection due to a mutation of the ZAP-70 gene causes autoimmune arthritis in mice. *Nature* 426, 454-460.

Sakaguchi, S., and Sakaguchi, N. (2005). Animal models of arthritis caused by systemic alteration of the immune system. *Curr Opin Immunol* 17, 589-594.

Scapini, P., Hu, Y., Chu, C.L., Migone, T.S., Defranco, A.L., Cassatella, M.A., and Lowell, C.A. (2010). Myeloid cells, BAFF, and IFN-gamma establish an inflammatory loop that exacerbates autoimmunity in Lyn-deficient mice. *J Exp Med* 207, 1757-1773.

Siggs, O.M., Miosge, L.A., Yates, A.L., Kucharska, E.M., Sheahan, D., Brdicka, T., Weiss, A., Liston, A., and Goodnow, C.C. (2007). Opposing functions of the T cell receptor kinase ZAP-70 in immunity and tolerance differentially titrate in response to nucleotide substitutions. *Immunity* 27, 912-926.

Singer, G.G., and Abbas, A.K. (1994). The fas antigen is involved in peripheral but not thymic deletion of T lymphocytes in T cell receptor transgenic mice. *Immunity* 1, 365-371.

Singh, S.B., Davis, A.S., Taylor, G.A., and Deretic, V. (2006). Human IRGM induces autophagy to eliminate intracellular mycobacteria. *Science* 313, 1438-1441.

Szabo, S.J., Sullivan, B.M., Peng, S.L., and Glimcher, L.H. (2003). Molecular mechanisms regulating Th1 immune responses. *Annu Rev Immunol* 21, 713-758.

Tucci, M., Quatraro, C., Dammacco, F., and Silvestris, F. (2006). Interleukin-18

overexpression as a hallmark of the activity of autoimmune inflammatory myopathies. *Clinical and experimental immunology* 146, 21-31.

Waldman, M., and Madaio, M.P. (2005). Pathogenic autoantibodies in lupus nephritis. *Lupus* 14, 19-24.

Watanabe-Fukunaga, R., Brannan, C.I., Copeland, N.G., Jenkins, N.A., and Nagata, S. (1992). Lymphoproliferation disorder in mice explained by defects in Fas antigen that mediates apoptosis. *Nature* 356, 314-317.

Waters, S.T., McDuffie, M., Bagavant, H., Deshmukh, U.S., Gaskin, F., Jiang, C., Tung, K.S., and Fu, S.M. (2004). Breaking tolerance to double stranded DNA, nucleosome, and other nuclear antigens is not required for the pathogenesis of lupus glomerulonephritis. *J Exp Med* 199, 255-264.

Weening, J.J., D'Agati, V.D., Schwartz, M.M., Seshan, S.V., Alpers, C.E., Appel, G.B., Balow, J.E., Bruijn, J.A., Cook, T., Ferrario, F., *et al.* (2004). The classification of glomerulonephritis in systemic lupus erythematosus revisited. *Kidney Int* 65, 521-530.

Wiik, A.S., Hoier-Madsen, M., Forslid, J., Charles, P., and Meyrowitsch, J. (2010). Antinuclear antibodies: a contemporary nomenclature using HEp-2 cells. *J Autoimmun* 35, 276-290.

Wu, X., Hou, W., Sun, S., Bi, E., Wang, Y., Shi, M., Zang, J., Dong, C., and Sun, B. (2006). Novel function of IFN-gamma: negative regulation of dendritic cell migration and T cell priming. *J Immunol* 177, 934-943.

Wuthrich, R.P., Yui, M.A., Mazoujian, G., Nabavi, N., Glimcher, L.H., and Kelley, V.E. (1989). Enhanced MHC class II expression in renal proximal tubules precedes loss of renal function in MRL/lpr mice with lupus nephritis. *Am J Pathol* 134, 45-51.

Xavier, R.M., Yamauchi, Y., Nakamura, M., Tanigawa, Y., Ishikura, H., Tsunematsu, T., and Kobayashi, S. (1995). Antinuclear antibodies in healthy aging people: a prospective study. *Mech Ageing Dev* 78, 145-154.

Yang, J.Q., Wen, X., Liu, H., Folayan, G., Dong, X., Zhou, M., Van Kaer, L., and Singh, R.R. (2007). Examining the role of CD1d and natural killer T cells in the development of nephritis in a genetically susceptible lupus model. *Arthritis Rheum* 56, 1219-1233.

Yoshitomi, H., Sakaguchi, N., Kobayashi, K., Brown, G.D., Tagami, T., Sakihama, T., Hirota, K., Tanaka, S., Nomura, T., Miki, I., *et al.* (2005). A role for fungal β -glucans and their receptor Dectin-1 in the induction of autoimmune arthritis in genetically susceptible mice. *J Exp Med* 201, 949-960.

Yu, P., Wellmann, U., Kunder, S., Quintanilla-Martinez, L., Jennen, L., Dear, N., Amann, K., Bauer, S., Winkler, T.H., and Wagner, H. (2006). Toll-like receptor 9-independent aggravation of glomerulonephritis in a novel model of SLE. *Int Immunol* 18, 1211-1219.

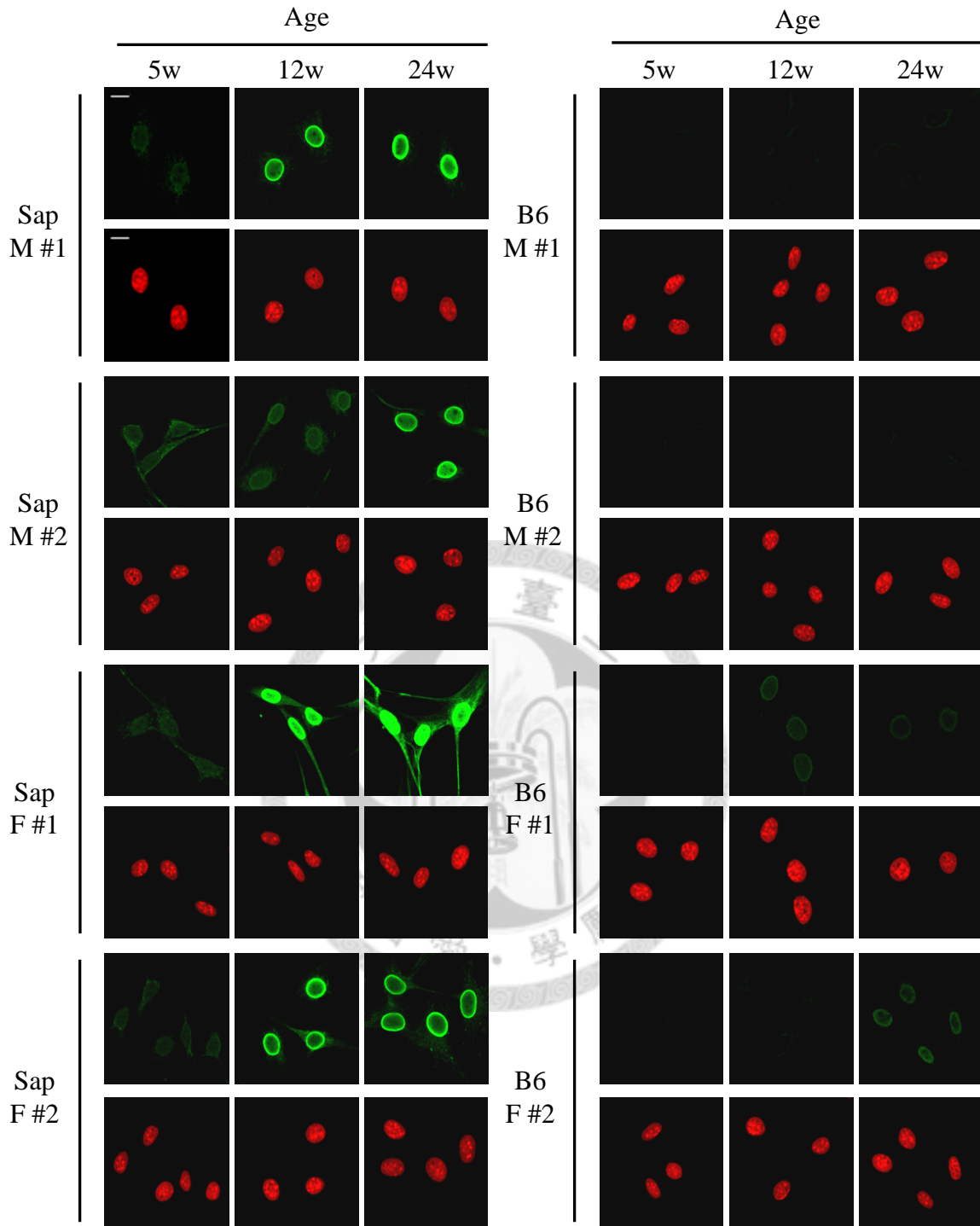


Figure 1. Appearance of autoantibodies in young Sap mice.

Tissue culture grown B16-F10 melanoma cells were fixed and incubated with serum samples (1:500 diluted) collected from two female (F) and two male (M) Sap and B6 mice longitudinally at indicated ages. Bound antibodies were detected by A488-conjugated anti-mouse Ig (green). Hoechst 33342 was used to detect the nucleus (red). The stained melanoma cells were analyzed by confocal microscopy. Images shown were taken at 630x magnification, 2x zoom. Scale bar = 10 μ m. The detailed procedure is as described in Materials and Methods section 2.3.

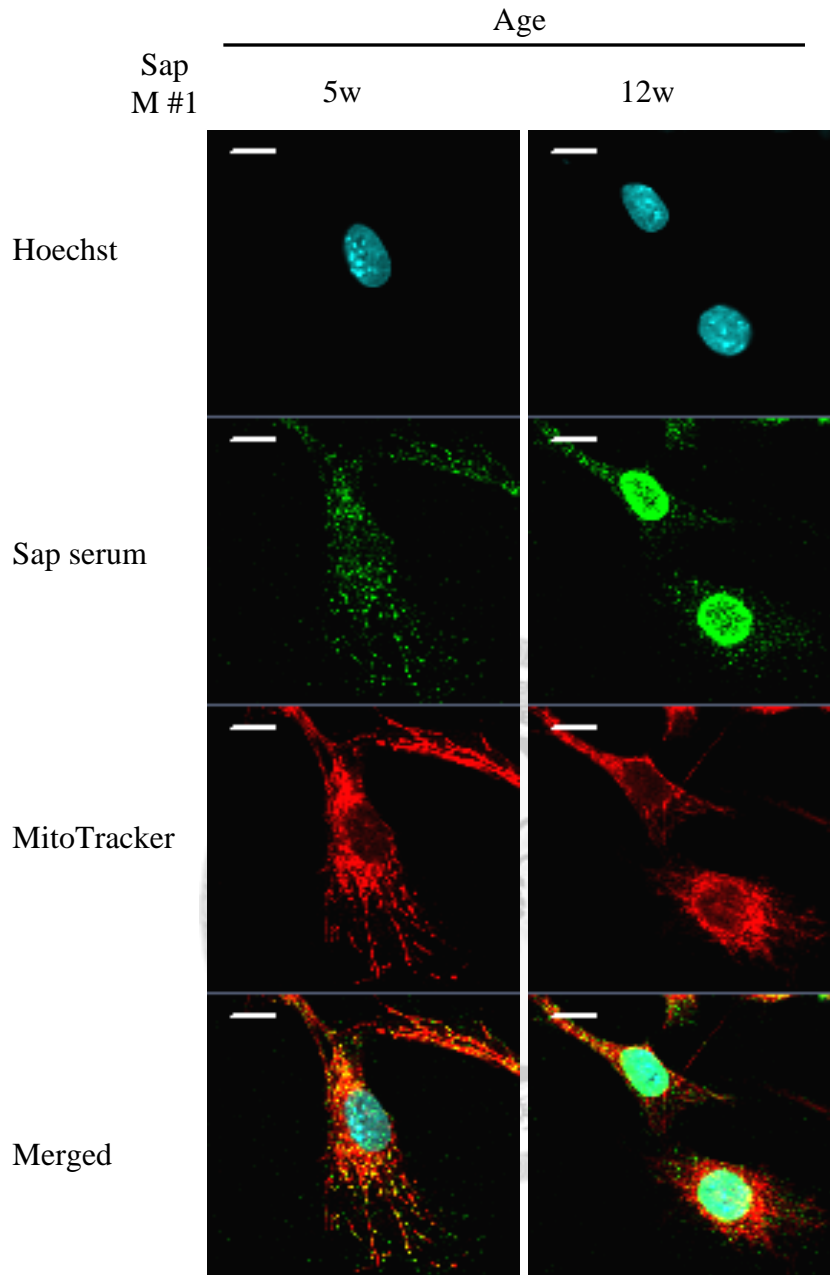


Figure 2. Co-localization of cytoplasmic staining pattern with mitochondrial marker.

Tissue culture grown B16-F10 melanoma cells were labeled with a mitochondrial marker (red). The cells were then fixed, permeabilized, and incubated with serum samples (1:500 diluted) collected from a male (M) Sap mouse at 5 weeks and 12 weeks of age. Bound antibodies were detected by A488-conjugated anti-mouse Ig (green). Hoechst 33342 was used to detect the nucleus (cyan). Immunofluorescence co-localization (yellow) of mouse Ig and mitochondrial marker was shown in the merged images. The cells were analyzed by confocal microscopy (630x magnification, 2x zoom, scale bars = 10 μ m). The detailed procedure is as described in Materials and Methods section 2.5.

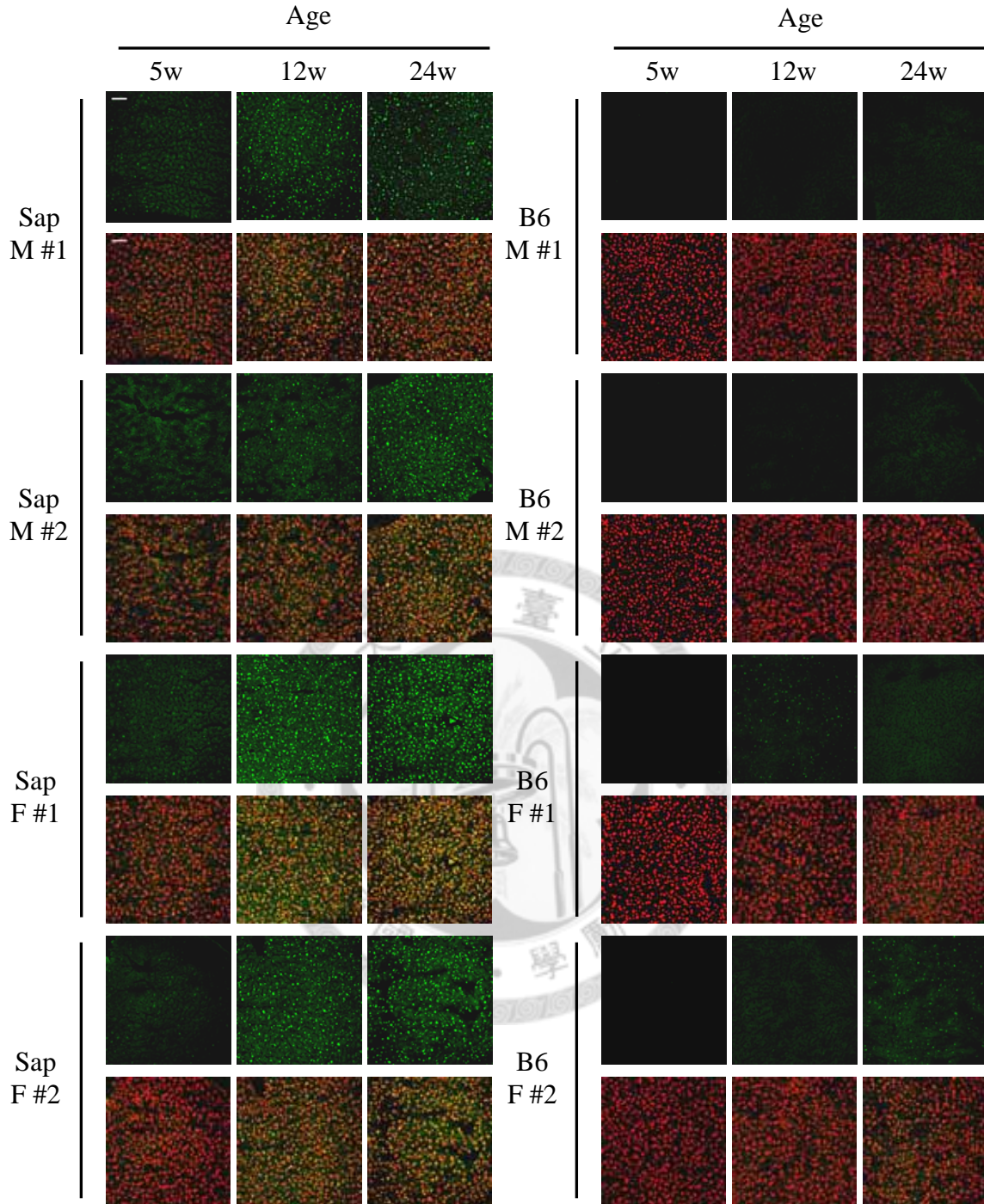


Figure 3. Appearance of autoantibodies in young Sap mice.

Liver frozen sections (5 μ m) from IgH-KO mice were fixed and incubated with serum samples (1:500 diluted) collected from two female (F) and two male (M) Sap and B6 mice longitudinally at indicated ages. Bound antibodies were detected by A488-conjugated anti-mouse Ig (green). Hoechst 33342 was used to detect the nucleus (red). Immunofluorescence co-localization (orange and yellow) of mouse Ig and nucleus was shown in merged images. The stained liver frozen sections were analyzed by confocal microscopy (200x magnification, scale bars = 50 μ m). The detailed procedure is as described in Materials and Methods section 2.4.

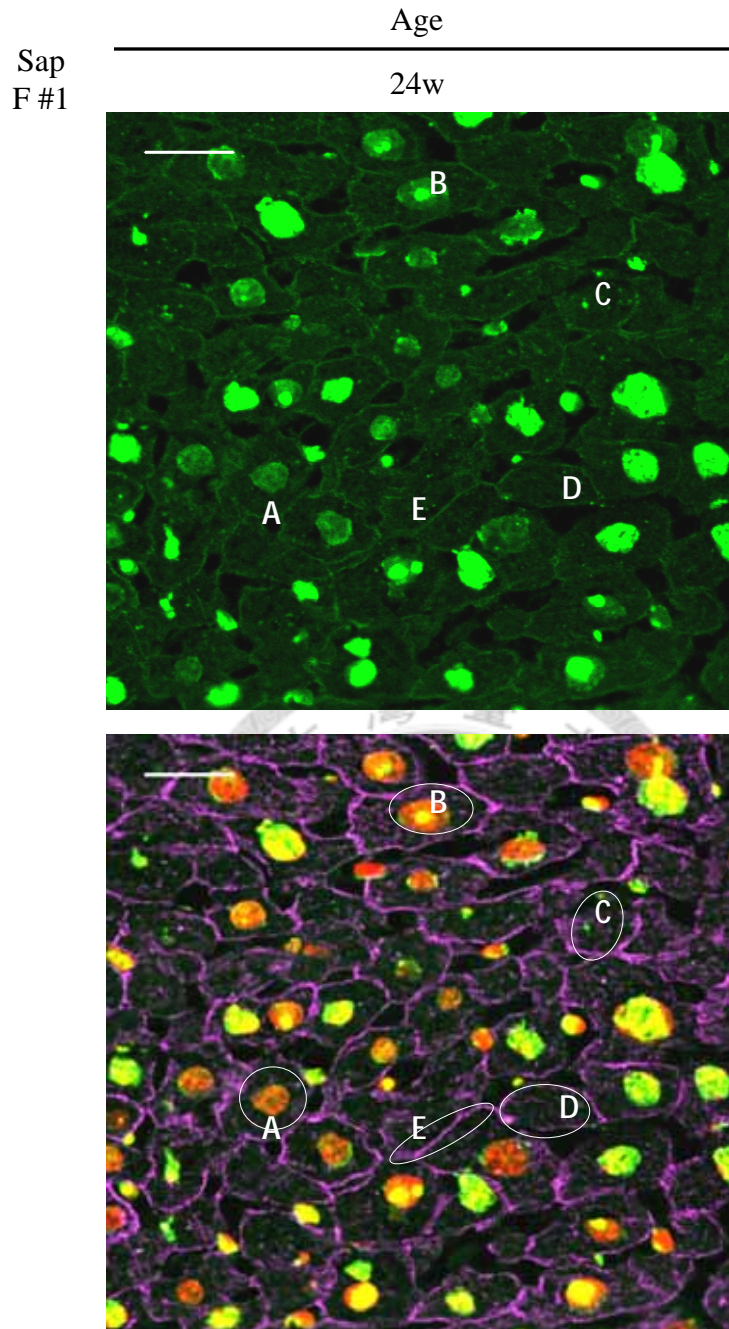


Figure 4. Five autoantibody staining patterns are defined by Sap autoantibody.

Liver frozen sections (5 μ m) from IgH-KO mice were fixed and incubated with serum samples (1:500 diluted) collected from a female Sap mouse at 24 weeks of age. Bound antibodies were detected by A488-conjugated anti-mouse Ig (green). Liver pancytokeratin were stained with A546-PanCK. Hoechst 33342 was used to detect the nucleus (red). Immunofluorescence co-localization (orange and yellow) of mouse Ig and nucleus was shown in the merged image: nuclear (A), nucleolar-like (B), cytoplasmic dot-like (C), cytoplasmic (D), and membranous (E) patterns. Stained liver frozen sections were analyzed by confocal microscopy (630x magnification, scale bars = 20 μ m). The detailed procedure is as described in Materials and Methods section 2.4.

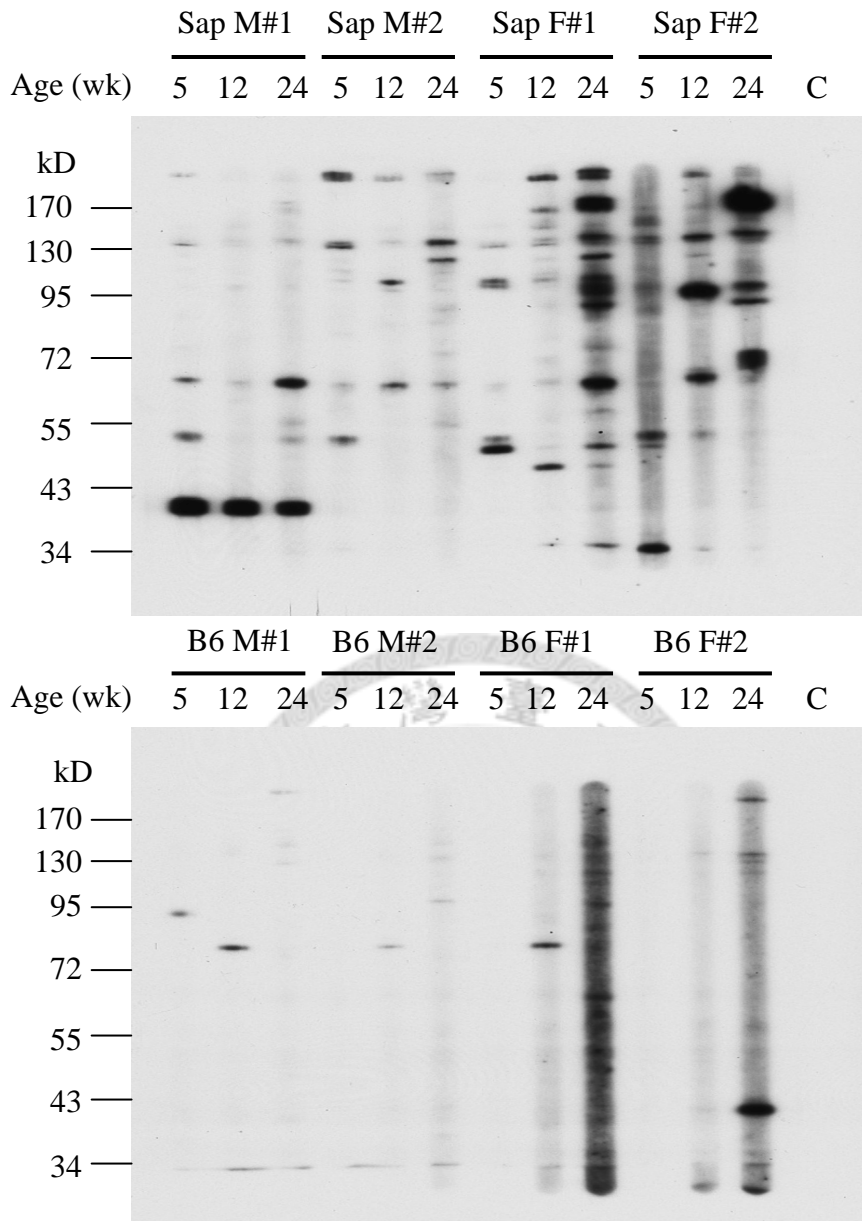


Figure 5. Western blotting of IgH-KO liver lysates reveals constant and changing autoantibody reactivity patterns.

IgH-KO liver lysates (0.065 mg protein per lane) were separated by SDS-PAGE polyacrylamide gel and followed by electrotransferring to a nitrocellulose membrane. The membrane was probed with indicated mouse serum samples (1:160 diluted) collected from two female (F) and two male (M) Sap and B6 mice longitudinally at indicated ages followed by immunoblotting with HRP-goat anti-mouse IgG (1:5000 diluted). A lane blotted with HRP-goat anti-mouse IgG without mouse serum was used as a control (lane C). Molecular weight markers (Kd) are as indicated. The detailed procedure is as described in Materials and Methods section 2.6.

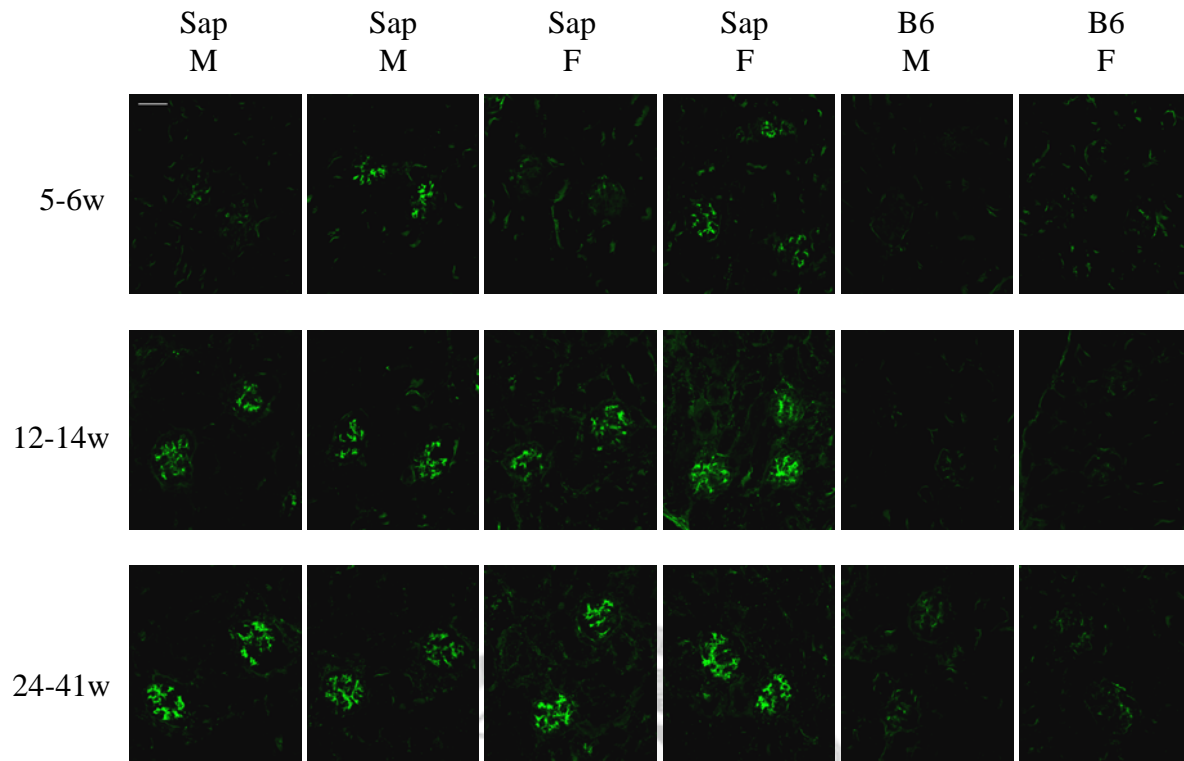


Figure 6. Immune complex deposition in kidney glomerulus.

Kidney frozen sections (5 μ m thickness) from two female (F) Sap, two male (M) Sap, one F B6, and one M B6 mice at indicated ages groups were examined for immune complex deposition. Kidney frozen sections were fixed and stained with A488 goat anti-mouse Ig (green). Deposition of immune complex in glomeruli was visualized by confocal microscopy (200x magnification, 1.5x zoom, scale bars = 50 μ m). Detailed procedure is as described in Materials and Methods section 2.7.

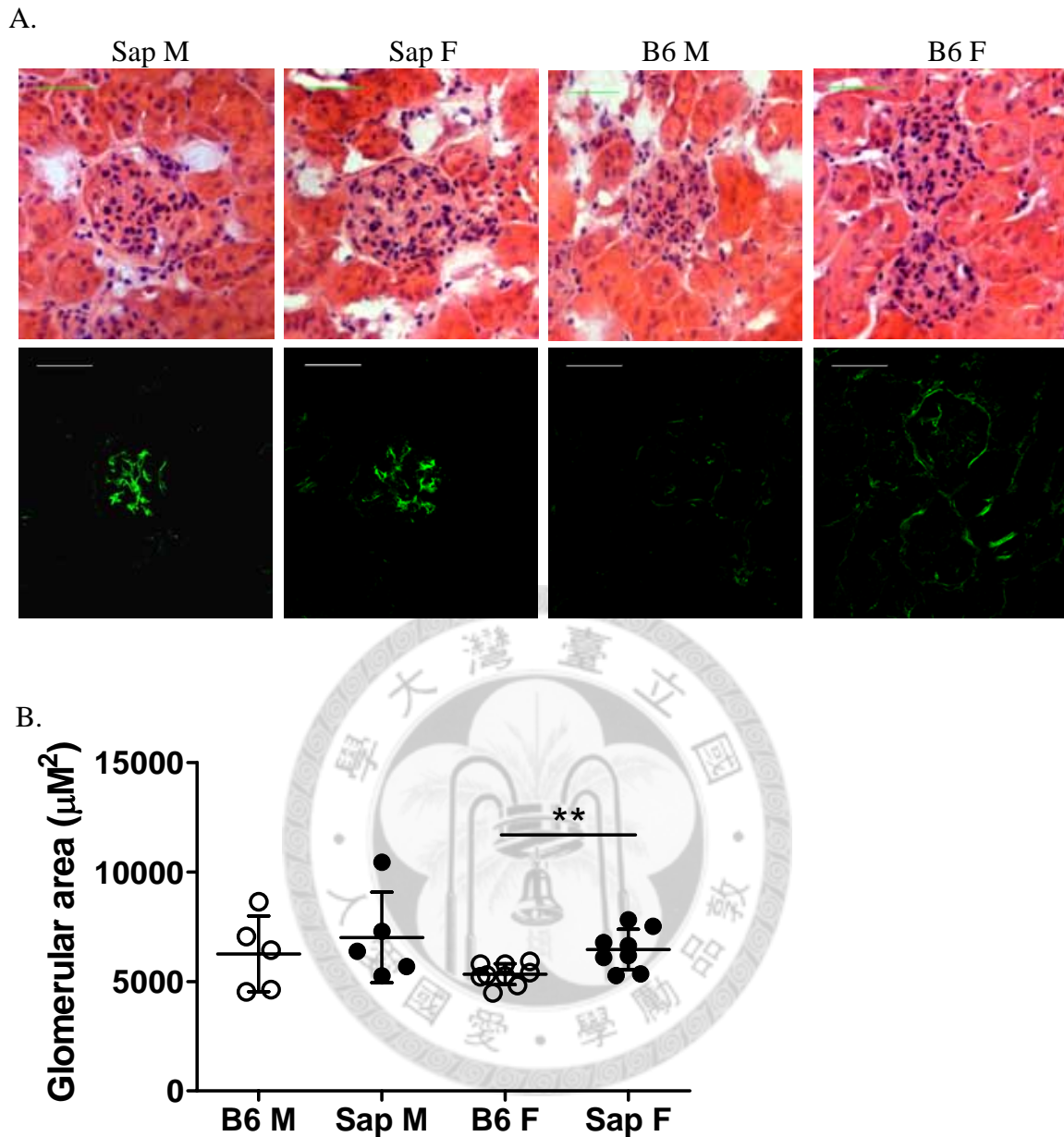


Figure 7. Glomerular immune complex deposition with enlarged glomeruli in Sap mice.

(A) Kidney serial frozen sections (5 μ m thickness) from a female (F) Sap, a male (M) Sap, a F B6, and a M B6 mice ranging from 24 to 41 wks of age were subjected to H&E staining (top row) or to staining with A488 goat anti-mouse Ig (bottom row). H&E images were taken using a Zeiss AxioZ1 Imager microscope (400x magnification). Immune complex deposition in glomeruli was analyzed by confocal microscopy (400x magnification, scale bars = 50 μ m). (B) Number of glomerulus counted: B6 M (n=5), Sap M (n=5), B6 F (n=9), Sap F (n=8). Each dot represents a single glomerulus, **P<0.01. The glomerular size was quantified with ZEN 2009 light edition. The detailed procedure is as described in Materials and Methods sections 2.7 and 2.8.

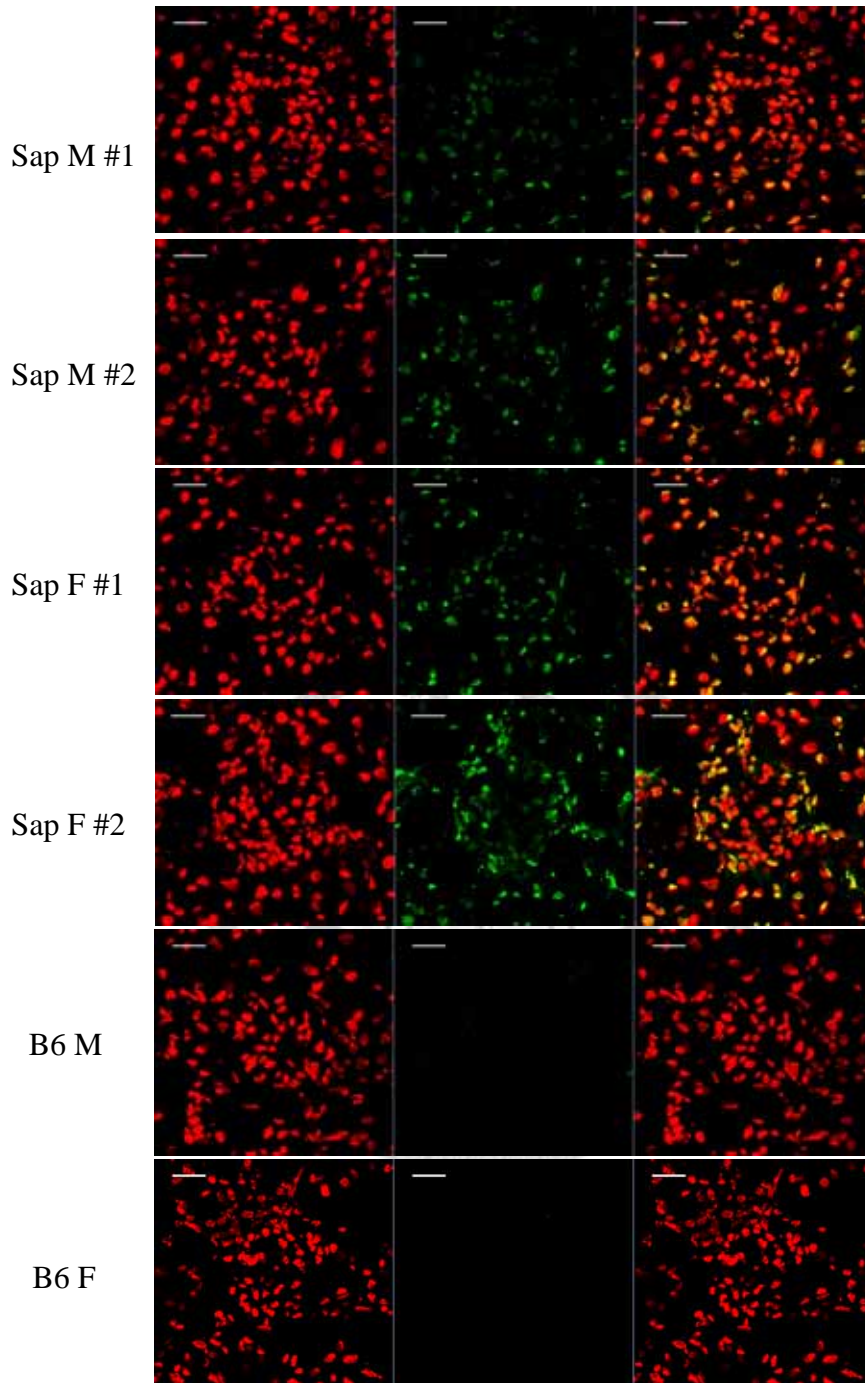


Figure 8. Sap autoantibodies do not bind to glomerular antigens.

Kidney frozen sections (5 μ m) from IgH-KO mice were fixed, permeabilized, and incubated with serum samples (1:500 dilution) collected from two male (M) Sap, two female (F) Sap, one M B6, and one F B6 mice ranging from 24 to 41 wks of ages. Bound antibodies were detected by A488-conjugated anti-mouse Ig (green). Hoechst 33342 was used to detect the nucleus (red). The overlay images indicated double positive cells in yellow. The stained kidney sections were analyzed by confocal microscopy. Images shown were taken at 630x magnification. Scale bar = 20 μ m. The detailed procedure is as described in Materials and Methods section 2.4.

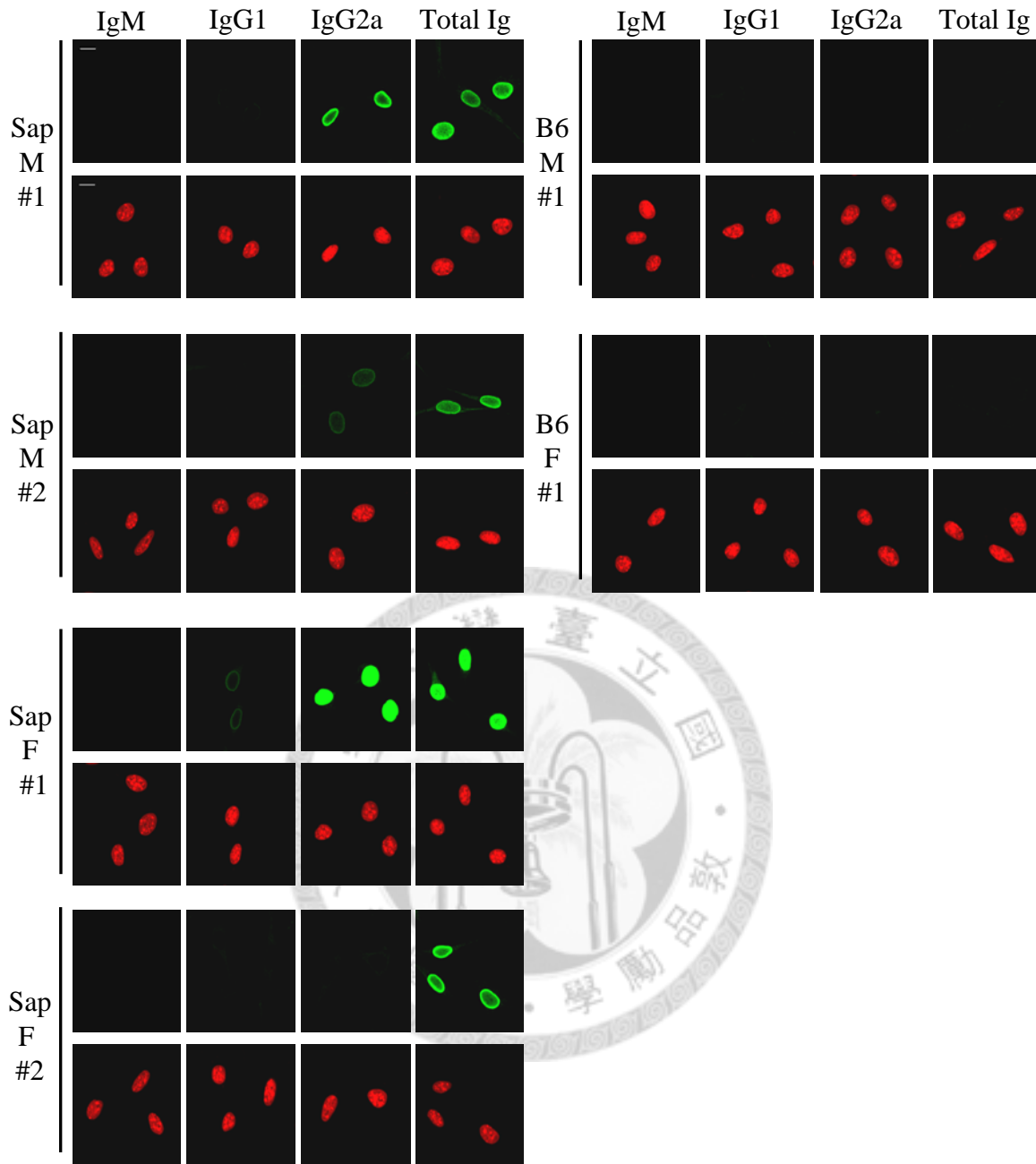


Figure 9. Sap B cells are able to class switch to IgG1 and IgG2a pathogenic autoantibodies.

Tissue culture grown B16-F10 melanoma cells were fixed and incubated with serum (1:500 diluted) samples collected from two female (F) Sap, two male (M) Sap, one F B6, and one M B6 mice at 24 weeks of ages. Bound antibodies were detected by A488-conjugated anti-mouse IgM, A488-conjugated anti-mouse Ig, or biotin rat anti-mouse IgG1 and IgG2a followed by detection with A488-SA (green). Hoechst 33342 was used to detect the nucleus (red). The stained melanoma cells were analyzed by confocal microscopy. Images shown were taken at 630x magnification, 2x Zoom. Scale bars = 10 μ m. Detailed procedure is as described in Materials and Methods section 2.3.

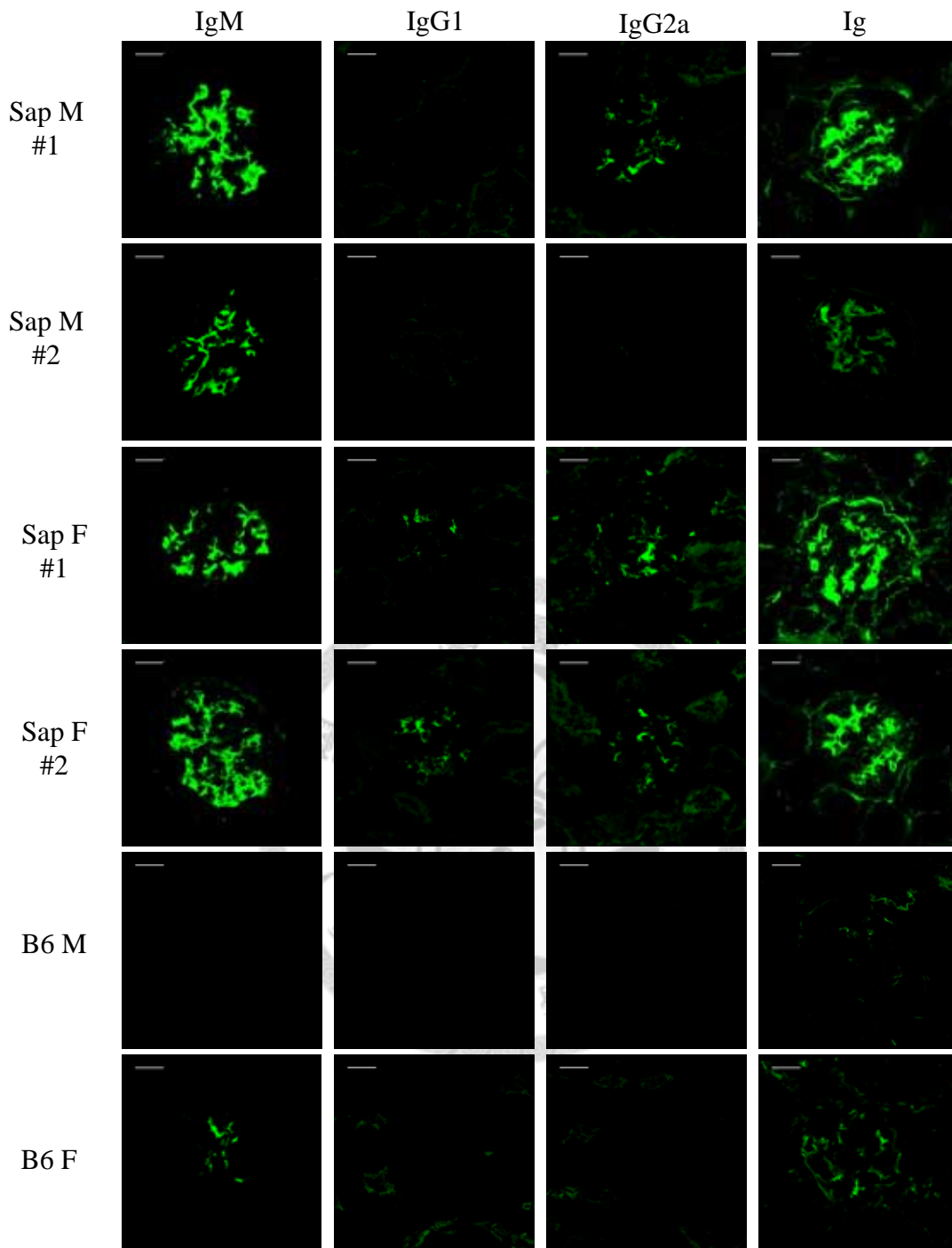


Figure 10. Glomerular immune complex deposition in Sap mice is mostly composed of autoantigen bound by autoantibody of IgM isotype.

Kidney frozen sections (5 μ m thickness) from two female (F) Sap, two male (M) Sap, one F B6, and one M B6 mice at ages ranging from 24 to 41 weeks were fixed and stained with A488 goat anti-mouse Ig, A488 rat anti-mouse IgM, or biotin rat anti-mouse IgG1 or IgG2a followed by detection of A488-SA as indicated (green). Deposition of immune complexes in glomeruli was visualized by confocal microscopy (630x magnification, scale bars = 20 μ m). Detailed procedure is as described in Materials and Methods section 2.7.

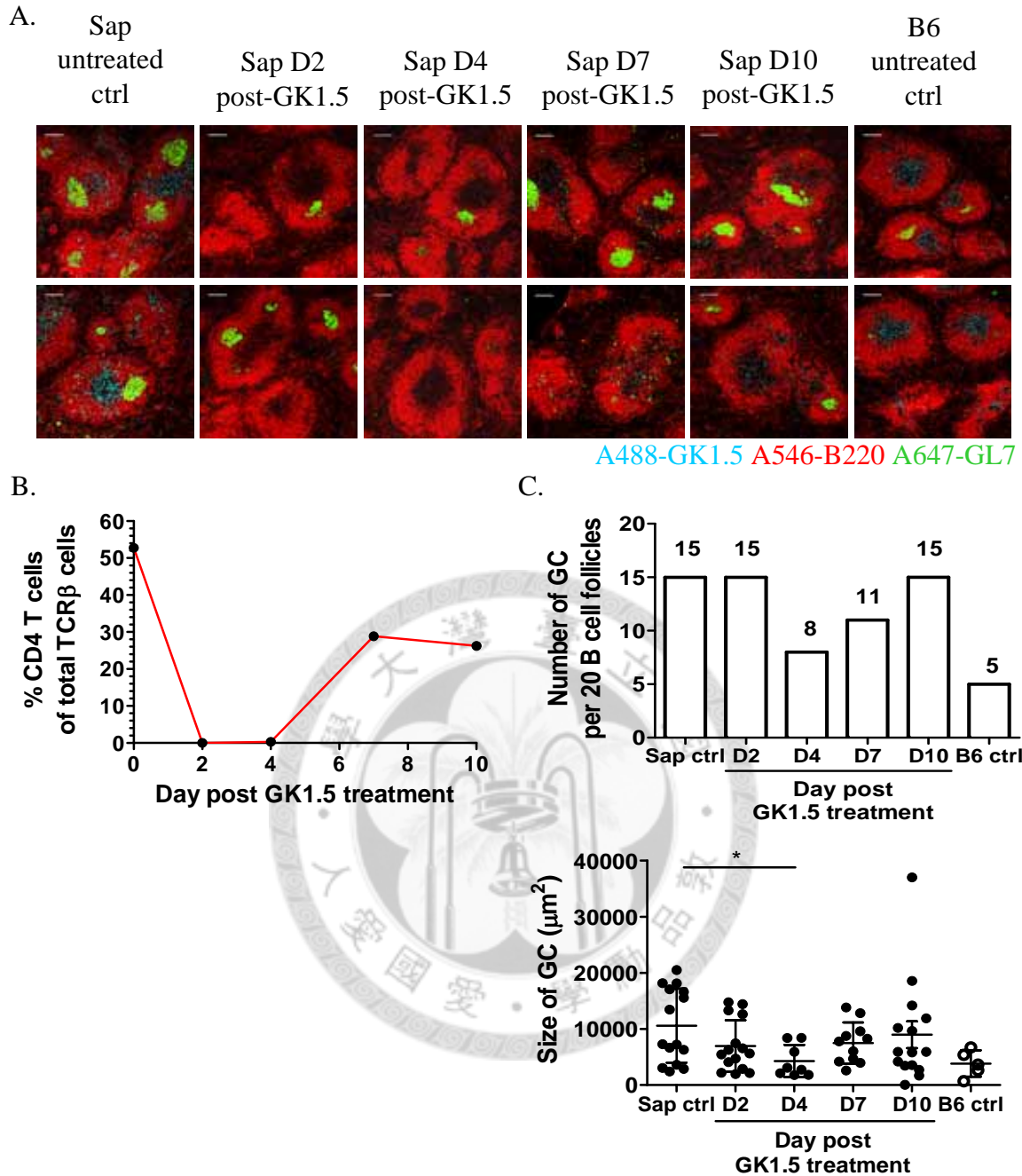


Figure 11. CD4⁺ T cell depletion results in rapid disappearance of germinal centers. Sap male mice (n=4, 12 wks of age) were treated with 200 μg GK1.5 mAb (i.v.). On indicated days post-GK1.5 treatment, spleens were removed. Single cell suspension from part of the spleen (~1/3) was subjected to marker analysis by flow cytometry. Frozen sections (5 μm thickness) made from the remainder of the spleens (~2/3) were stained with A488-GK1.5, A546-B220, A647-GL7, and Fc blocker 2.4G2 to identify germinal centers. (A) Germinal centers defined by GL7⁺ cell clusters within B220⁺ B cell follicles were analyzed by confocal microscopy (100x magnification, scale bars = 100 μm). (B) Percentages of CD4⁺ T cells within TCR^β⁺ cells in the indicated mouse spleens. (C) A total of 20 B cell follicles were examined and the number and size of germinal centers found in these 20 B cell follicles were shown, *P<0.05. Detailed procedure is as described in Materials and Methods sections 2.7, 2.9 and 2.10.

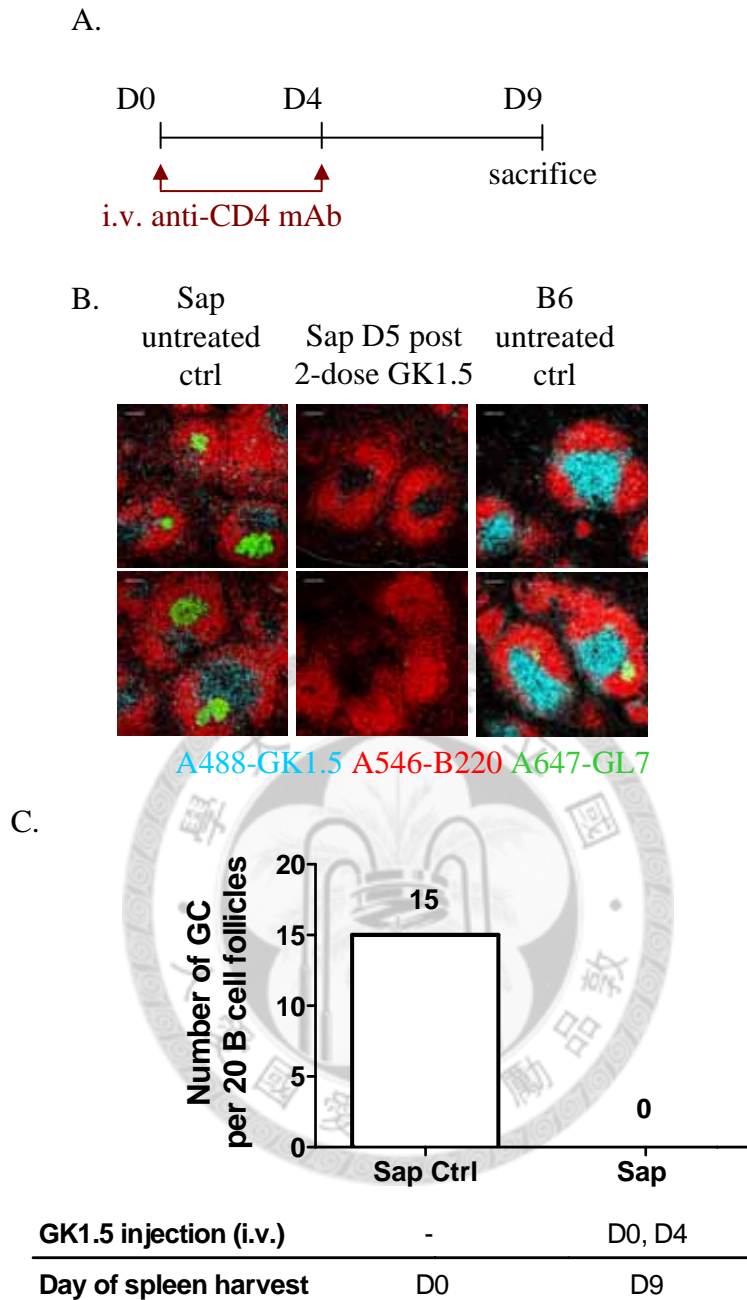


Figure 12. 2-dose *in vivo* CD4⁺ T cell depletion leads to complete disappearance of germinal centers.

Sap male mouse (n=1, 12-13 wks of age) was repeatedly treated with 200 μ g GK1.5 mAb (i.v.) on indicated days. Spleens were removed 5 days post-GK1.5 treatment. Spleen frozen sections (5 μ m thickness) were prepared and stained with A488-GK1.5, A546-B220, A647-GL7, and Fc blocker 2.4G2 to identify germinal centers. (A) Experiment design for 2-dose anti-CD4 mAb treatment. (B) Germinal centers defined by GL7⁺ cell clusters within B220⁺ B cell follicles were analyzed by confocal microscopy (100x magnification, scale bars = 100 μ m). (C) A total of 20 B cell follicles were examined and the number of germinal centers found in these 20 B cell follicles were shown. Detailed procedure is as described in Materials and Methods sections 2.7 and 2.9.

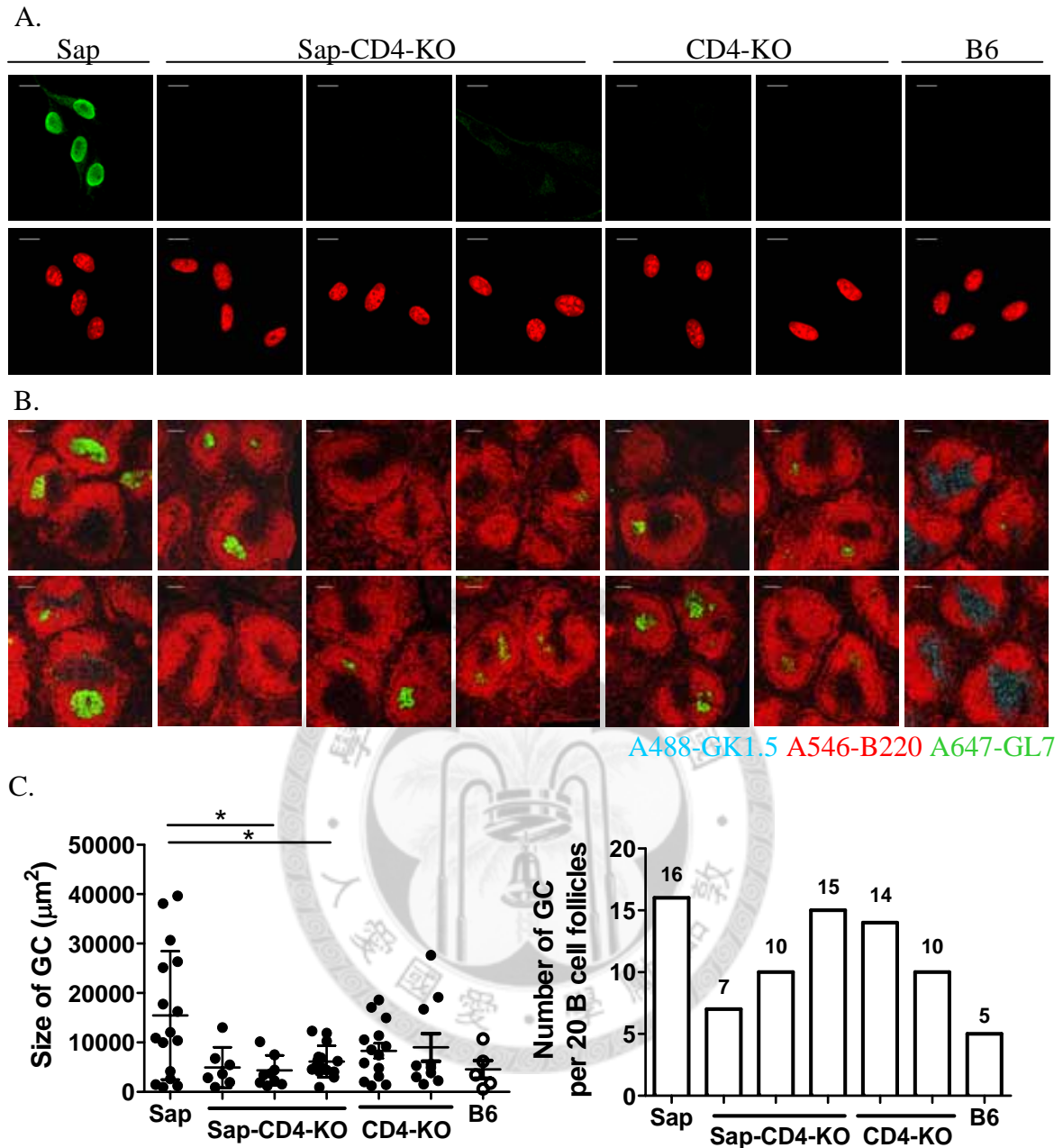


Figure 13. Greatly diminished autoantibody production but not GC formation in Sap-CD4-KO mice.

Serum samples were collected from one male (M) Sap, one M B6, one M and two female (F) Sap-CD4-KO mice, and one M and one F CD4-KO mice at ages ranging from 12- to 14-wks. Spleen frozen sections (5 μ m thickness) were prepared and stained with A488-GK1.5, A546-B220, A647-GL7, and Fc blocker 2.4G2 to identify germinal centers. (A) Cultured and fixed B16-F10 cells stained with sera (1:500 dilution) from the indicated mice. (630x magnification, 2x zoom, scale bars = 10 μ m). (B) Germinal centers defined by GL7⁺ cell clusters within B220⁺ B cell follicles were analyzed by confocal microscopy (100x magnification, scale bars = 100 μ m). (C) A total of 20 B cell follicles were examined and the number and size of germinal centers found in these 20 B cell follicles were shown, *P<0.05. Detailed procedure is as described in Materials and Methods sections 2.3 and 2.7.

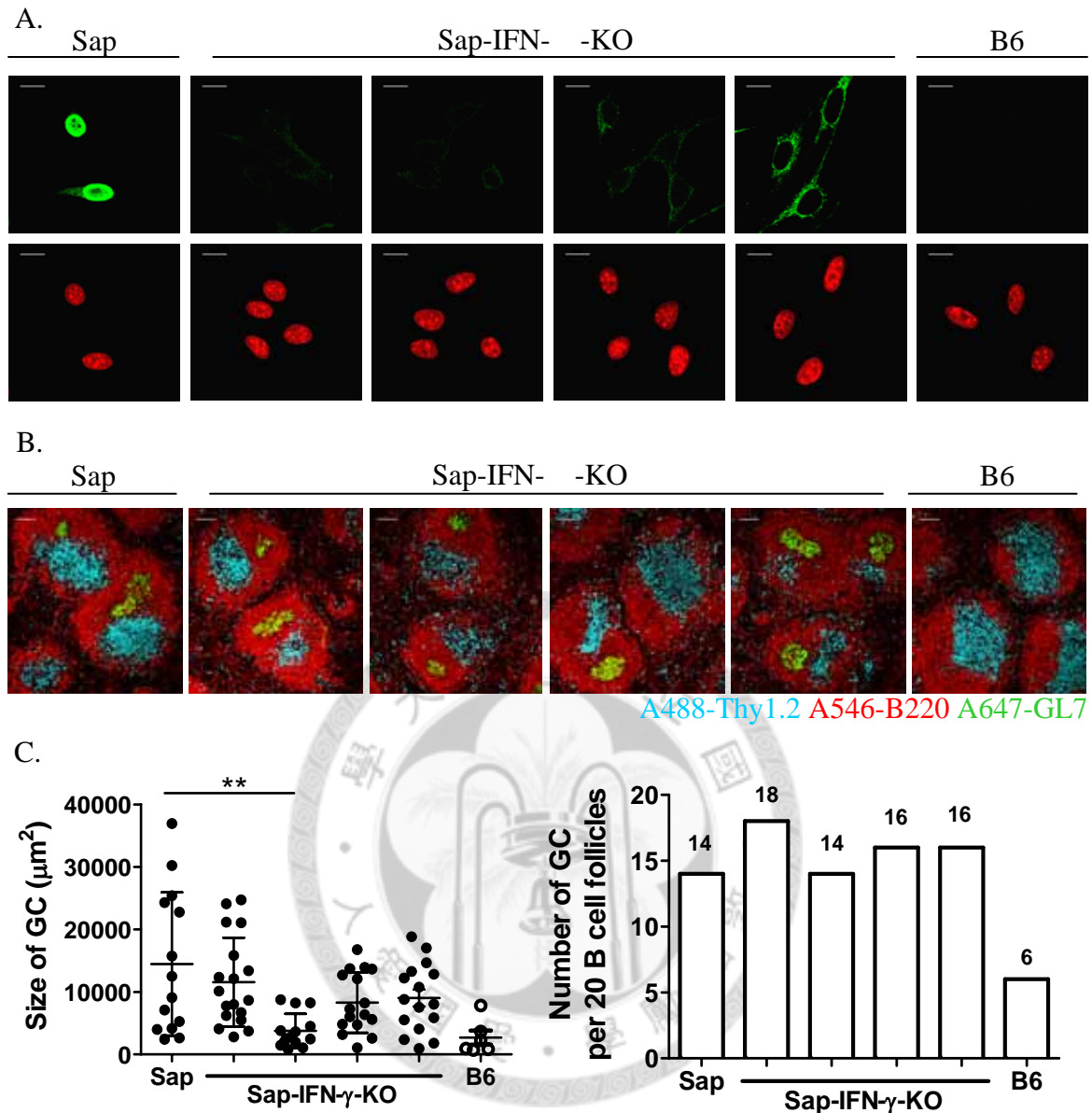


Figure 14. Loss of anti-nuclear but not anti-cytoplasmic autoantibodies, and reduced number of splenic germinal centers in Sap-IFN- γ -KO mice.

Serum samples and spleens were collected from Sap male (M) mouse (n=1, 12 wks of age), Sap-IFN- γ -KO M mouse (n=4, 12-14 wks of age), and B6 M mouse (n=1, 12 wks of age). Spleen sections (5 μm thickness) were prepared and stained with A488-Thy1.2, A546-B220, A647-GL7, and Fc blocker 2.4G2 to identify germinal centers. (A) Cultured and fixed B16-F10 cells stained with sera (1:500 dilution) from the indicated mice (630x magnification, 2x zoom, scale bars = 10 μm). (B) Germinal centers defined by GL7⁺ cell clusters within B220⁺ B cell follicles were analyzed by confocal microscopy (100x magnification, scale bars = 100 μm). (C) A total of 20 B cell follicles were examined and the number and size of germinal centers found in these 20 B cell follicles were shown, **P<0.01. Detailed procedure is as described in Materials and Methods sections 2.3 and 2.7.

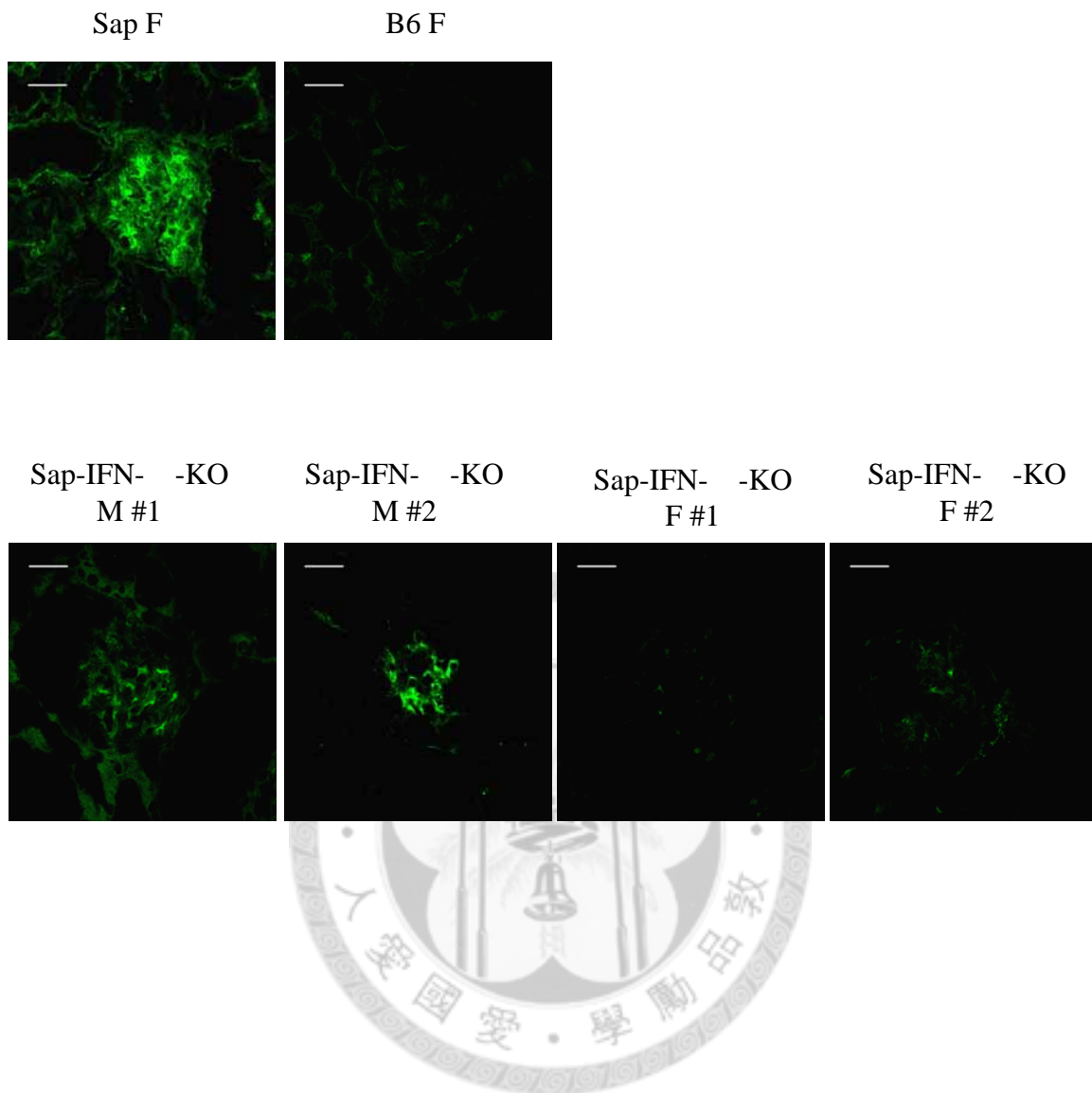


Figure 15. Glomerular immune complex deposition is greatly reduced in Sap-IFN- γ -KO mice.

Kidney frozen sections (5 μ m thickness) from one female (F) Sap, two male (M) and two F Sap-IFN- γ -KO, and one F B6 mice at ages ranging from 12- to 14-wks, were fixed and stained with A488 goat anti-mouse Ig (green) for immune complex deposition. Deposition of immune complexes in glomeruli was visualized by confocal microscopy (630x magnification, scale bars = 20 μ m). Detailed procedure is as described in Materials and Methods section 2.7.

Sap-IFN- γ -KO

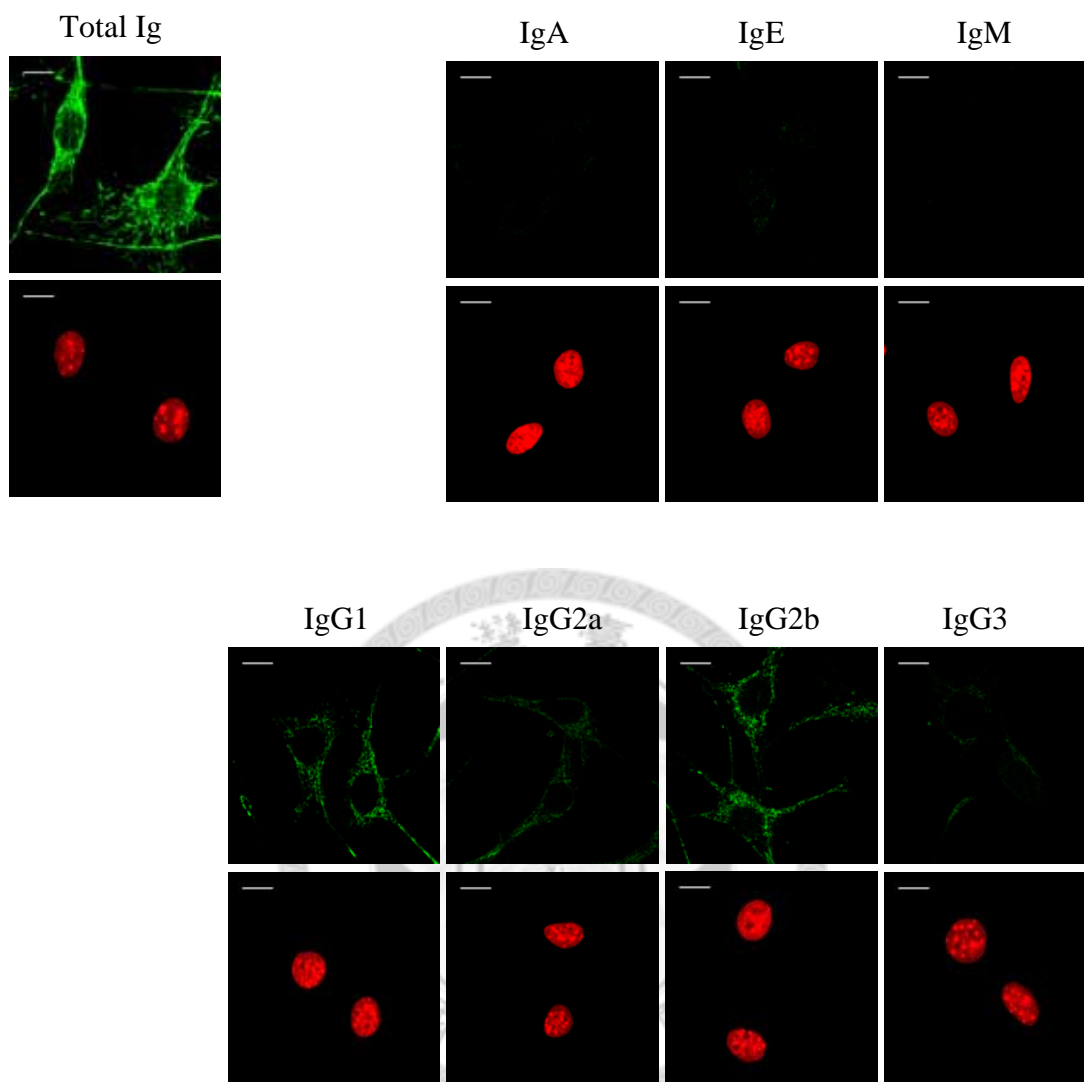


Figure 16. Predominance of IgG1 and IgG2b subclasses of anti-cytoplasmic autoantibodies in Sap-IFN- γ -KO mice.

Tissue culture grown B16-F10 melanoma cells were fixed and incubated with serum samples (1:500 diluted) collected from one female Sap-IFN- γ -KO mice at 23 weeks of ages. Bound antibodies were detected by A488-conjugated goat anti-mouse Ig, A488-conjugated rabbit anti-mouse IgM, or biotin rat anti-mouse IgA, IgE, IgG1, IgG2a, IgG2b, and IgG3 followed by detection with A488-SA (green). Hoechst 33342 was used to detect the nucleus (red). The stained melanoma cells were analyzed by confocal microscopy. Images shown were taken at 630x magnification, 2x Zoom. Scale bars = 10 μ m. Detailed procedure is as described in Materials and Methods section 2.3.

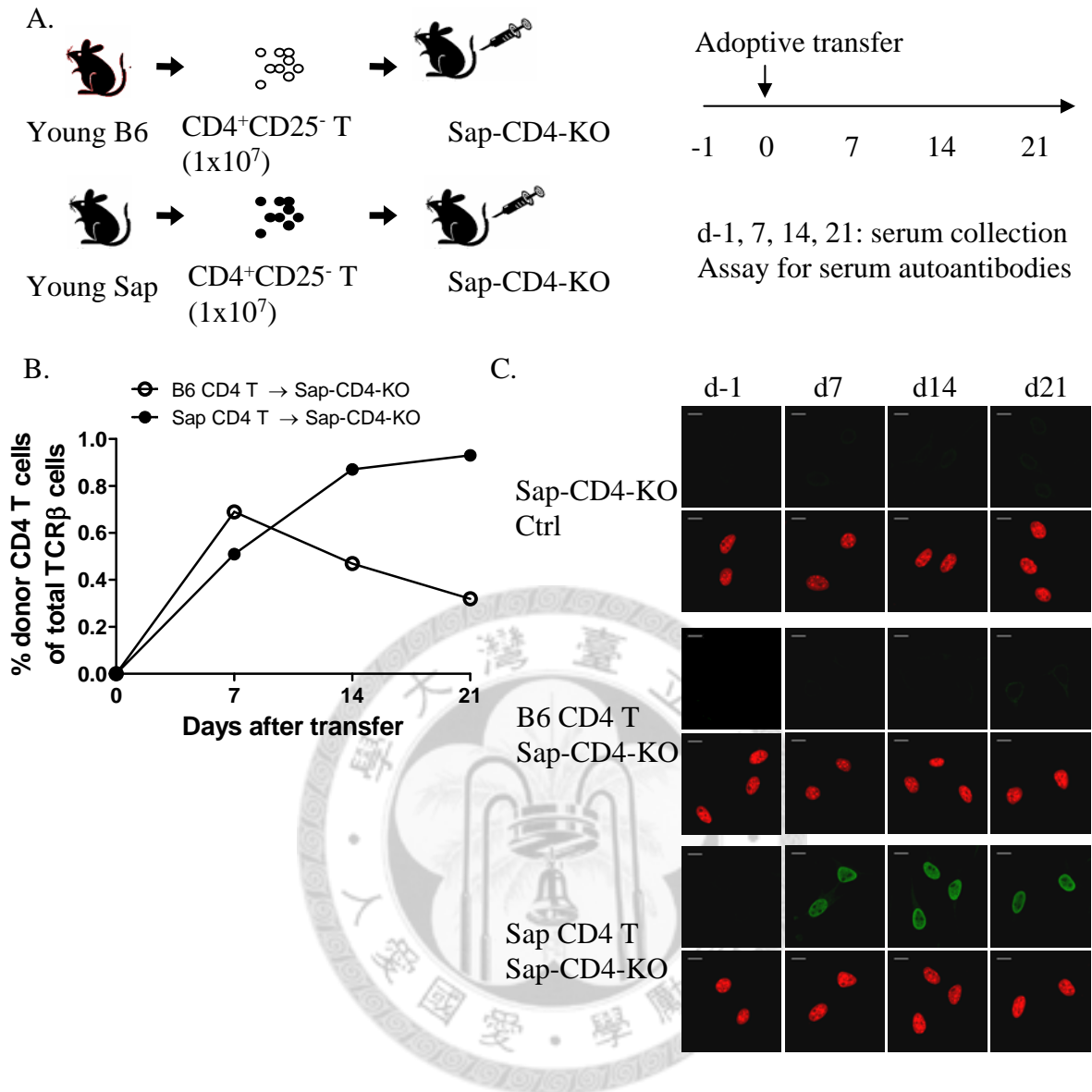


Figure 17. Adoptive transfer of $CD4^+$ T cells from young Sap mice or B6 mice to Sap-CD4-KO mice induce anti-nuclear but not anti-cytoplasmic autoantibodies.

Sort-purified $CD4^+$ T cells were isolated from the spleens of Sap or B6 mice (4 wks of age) and adoptively transferred into naive Sap-CD4-KO mice (12 wks of age). Sap-CD4-KO control mouse did not receive any transferred cells. (A) Study design of the adoptive transfer experiment. (B) Tracing of donor $CD4^+$ T cells by flow cytometry at indicated days. Percentages of donor $CD4^+$ T cells within TCR^+ cells in recipient PBL. (C) Tissue culture grown B16-F10 melanoma cells were fixed and incubated with serum samples (1:500 diluted) collected from the recipients at indicated days. Bound antibodies were detected by A488-conjugated anti-mouse Ig (green). Hoechst 33342 was used to detect the nucleus (red). The stained melanoma cells were analyzed by confocal microscopy. Images shown were taken at 630x magnification, 2x zoom. Scale bar = 10 μm . The detailed procedure is as described in Materials and Methods sections 2.3, 2.11, 2.12, 2.13, and 2.14.

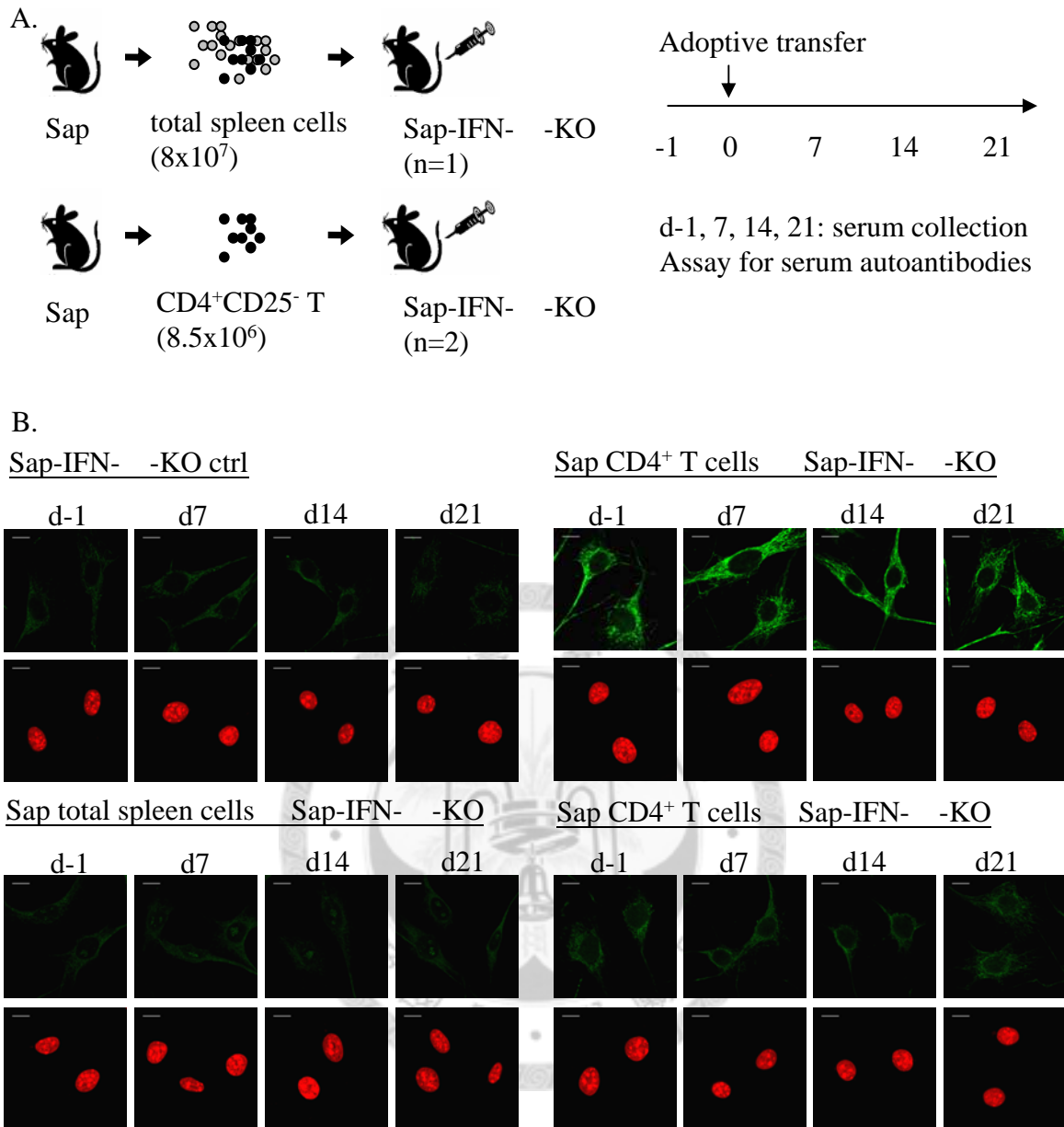


Figure 18. Transferring of total spleen cells or Sap CD4⁺ T cells from Sap mice to Sap-IFN- -KO mice fails to restore ANA production.

Total spleen cells or sort-purified CD4⁺ T cells were isolated from the spleens of Sap mice (12 wks of age) and adoptively transferred into naive Sap-IFN- -KO mice (23 wks of age). Sap-IFN- -KO control mice did not receive any transferred cells. (A) Study design of the adoptive transfer experiment. (B) Tissue culture grown B16-F10 melanoma cells were fixed and incubated with serum samples (1:500 diluted) collected from the recipients at indicated days. Bound antibodies were detected by A488-conjugated anti-mouse Ig (green). Hoechst 33342 was used to detect the nucleus (red). The stained melanoma cells were analyzed by confocal microscopy. Images shown were taken at 630x magnification, 2x zoom. Scale bar = 10 μ m. The detailed procedure is as described in Materials and Methods sections 2.3, 2.11, 2.12, and 2.13.

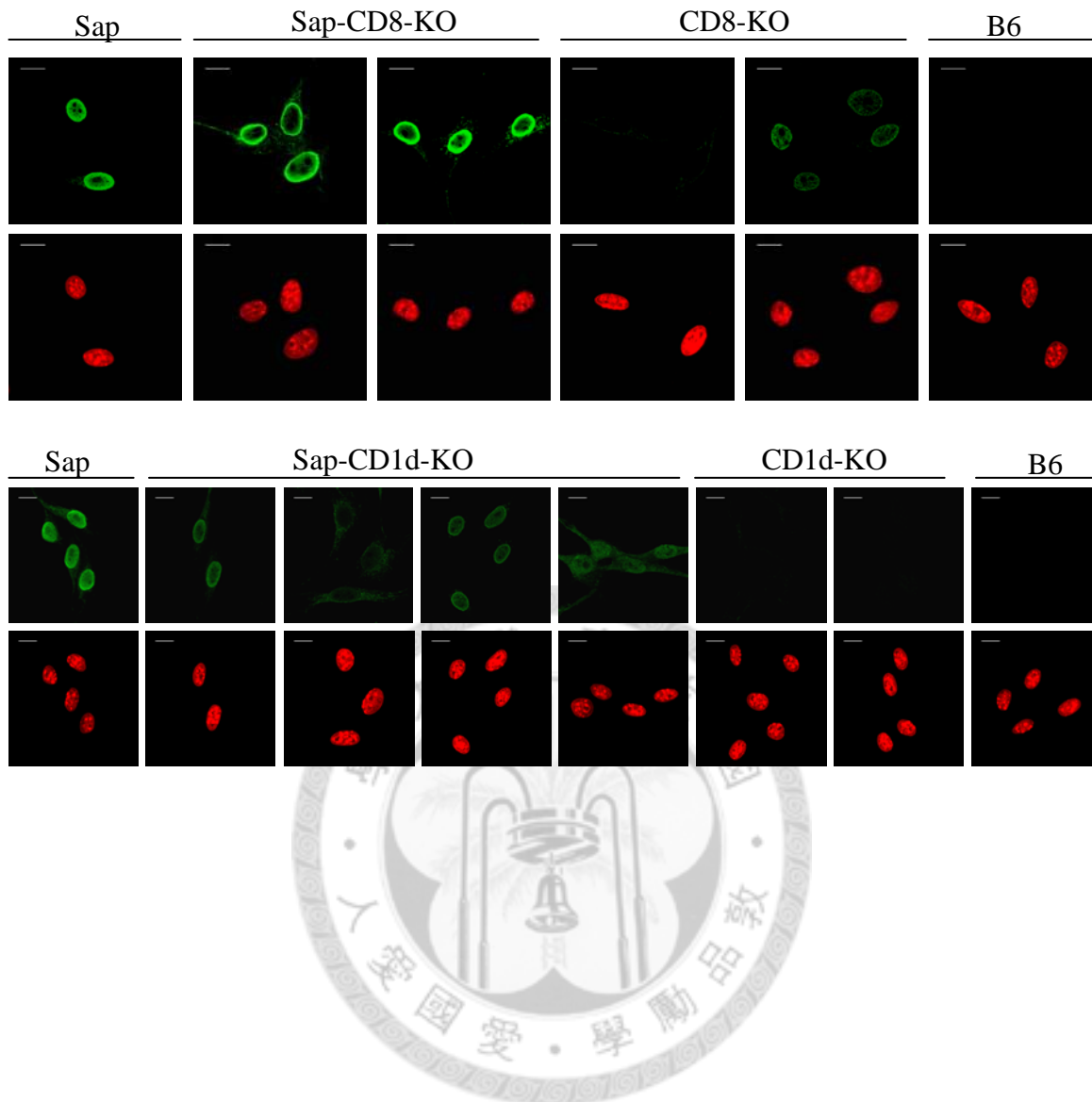


Figure 19. Autoantibody response in Sap mice is partially dependent on NKT cells but not CD8⁺ T cells.

Tissue culture grown B16-F10 melanoma cells were fixed and incubated with serum samples (1:500 diluted) collected from one male (M) Sap, two female (F) Sap-CD8-KO, one M and one F CD8-KO, two M and two F Sap-CD1d-KO, one M and one F CD1d-KO, and one M B6 mice at ages ranging from 12- to 14-wks. Bound antibodies were detected by A488-conjugated anti-mouse Ig (green). Hoechst 33342 was used to detect the nucleus (red). The stained melanoma cells were visualized by confocal microscopy (630x magnification, 2x zoom. Scale bar = 10 μ m). Detailed procedure is as described in Materials and Methods section 2.3.

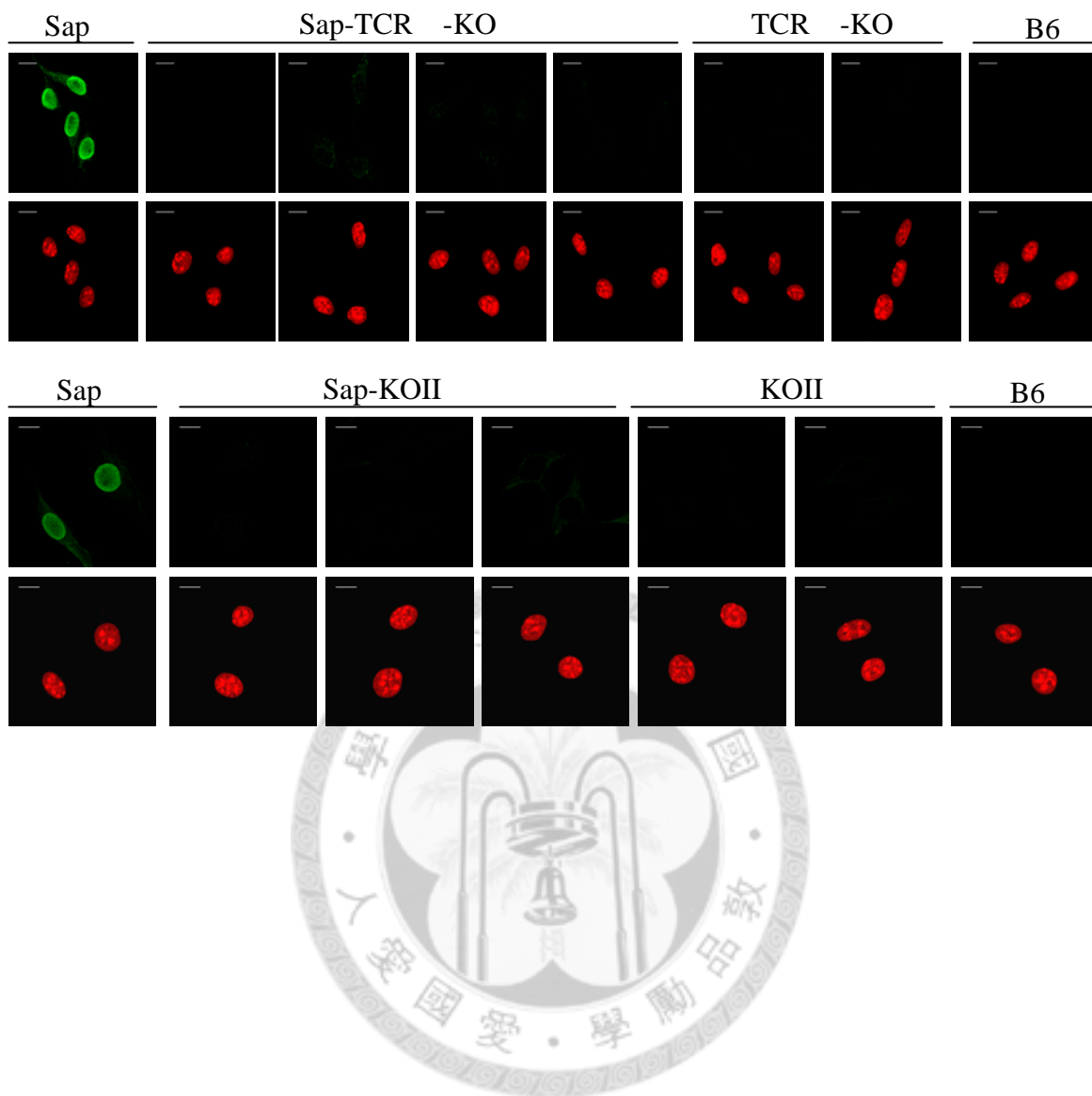


Figure 20. Screening of serum autoantibodies in Sap-TCR α -KO and Sap-KOII mice.

Tissue culture grown B16-F10 melanoma cells were fixed and incubated with serum samples (1:500 diluted) collected from Sap (n=1, M, 13 wks of age), Sap-TCR α -KO mice (n=4, 2M2F, 12-14 wks of age), TCR α -KO mice (n=2, 1M1F, 12-14 wks of age), Sap-KOII mice (n=3, 2M1F, 9-13 wks of age), KOII mice (n=2, 1M1F, 19 wks of age), and B6 mouse (n=1, M, 10 wks of age). Bound antibodies were detected by A488-conjugated anti-mouse Ig (green). Hoechst 33342 was used to detect the nucleus (red). The stained melanoma cells were visualized by confocal microscopy (630x magnification, 2x zoom). Scale bar = 10 μ m). Detailed procedure is as described in Materials and Methods section 2.3.

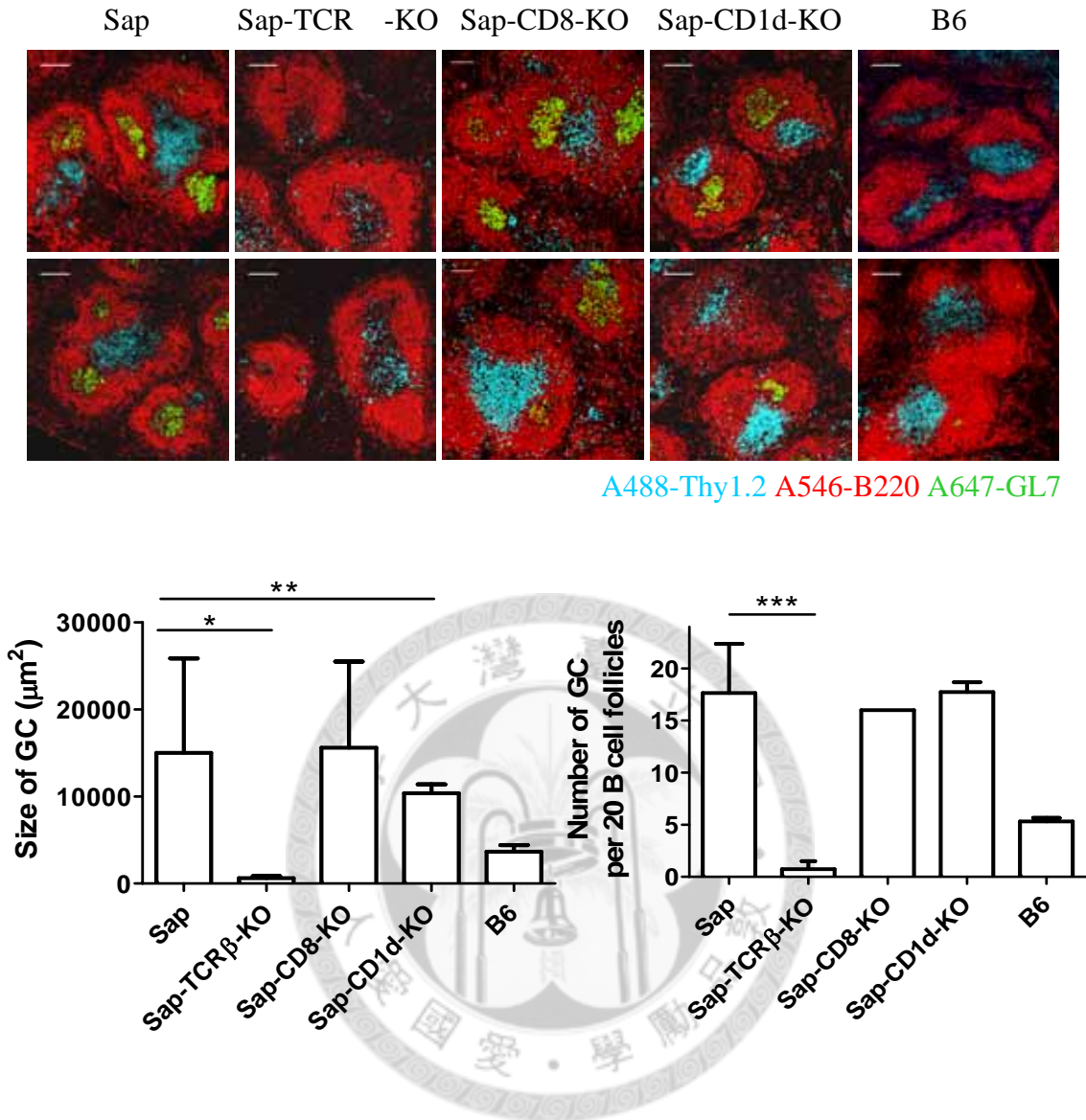


Figure 21. Analysis of formation of Germinal centers in Sap-TCR β -KO, Sap-CD8-KO, and Sap-CD1d-KO mice.

Spleen frozen sections from indicated mice were stained with A488-Thy1.2, A546-B220, and A647-GL7. Germinal centers defined by GL7⁺ cell clusters within B220⁺ B cell follicles were analyzed by confocal microscopy (100x magnification, scale bars = 100 μ m). A total of 20 B cell follicles were examined and the number and size of germinal centers found in these 20 B cell follicles of each mouse were shown. Graphs represent mean \pm SD. Each group consisted of one to four mice. *P<0.05, **P<0.01, ***P<0.001. Detailed procedure is as described in Materials and Methods section 2.7.